SUBMITTED TO THE *Astrophysical Journal*
Preprint typeset using LaTeX style AASTeX6 v. 1.0

YOUNG STARS WITH SALT

ADRIC R. RIEDEL
Department of Astronomy, California Institute of Technology, Pasadena, CA 91125

Department of Astrophysics, The American Museum of Natural History, New York, NY, 10024

Department of Engineering Science and Physics, The College of Staten Island, Staten Island, NY, 10314
and
Department of Physics and Astronomy, Hunter College, New York, NY, 10065

MUNAZZA K. ALAM
Department of Astronomy, Harvard University, Cambridge, MA 02138

Department of Astrophysics, The American Museum of Natural History, New York, NY, 10024
and
Department of Physics and Astronomy, Hunter College, New York, NY, 10065

EMILY L. RICE
Department of Engineering Science and Physics, The College of Staten Island, Staten Island, NY, 10314

Department of Astrophysics, The American Museum of Natural History, New York, NY, 10024
and
Physics Program, The Graduate Center, CUNY, New York, NY 10016

KELLE L. CRUZ
Department of Physics and Astronomy, Hunter College, City University of New York, New York, NY, 10065

Department of Astrophysics, The American Museum of Natural History, New York, NY, 10024
and
Physics Program, The Graduate Center, CUNY, New York, NY 10016

TODD J. HENRY
RECONS Institute, Chambersburg, PA.

ABSTRACT

We present a spectroscopic and kinematic analysis of 79 nearby M dwarfs in 77 systems. All are low-proper-motion southern hemisphere objects and were identified in a nearby star survey with a demonstrated sensitivity to young stars. Using low-resolution optical spectroscopy from the Red Side Spectrograph (RSS) on the South African Large Telescope (SALT), we have determined radial velocities, H-alpha, Lithium 6708Å, and Potassium 7699Å equivalent widths linked to age and activity, and spectral types for all our targets. Combined with astrometric information from literature sources, we identify 44 young stars. Eighteen are previously known members of moving groups within 100 parsecs of the Sun. Twelve are new members, including one member of the TW Hydra moving group, one member of the 32 Orionis moving group, nine members of Tucana-Horologium, one member of Argus, and two new members of AB Doradus. We also find fourteen young star systems that are not members of any known groups. The remaining 33 star systems do not appear to be young. This appears to be evidence of a new population of nearby young stars not related to the known nearby young

moving groups.

Keywords: stars:low-mass — stars:pre-main-sequence — open clusters and associations:general — galaxy:solar neighborhood — techniques:spectroscopic

1. INTRODUCTION

The Nearby Young Moving Groups (NYMGs), loose associations of nearby stars between 5 (ϵ Cha, Murphy et al. 2013) and 525 Myr old (χ^1 For, Pöhnl & Paunzen 2010), are thought to be remnants of small-scale star formation in the nearby Sco-Cen star forming region and represent the closest assemblages of pre-main-sequence stars and young planetary systems to the Sun. They are valuable targets for studying the formation of low mass stars, brown dwarfs, and planetary systems, because their proximity makes it easier to study fainter objects and companions at smaller separations.

A number of investigators have dedicated time to large-scale surveys for members of the nearby young moving groups (e.g. Torres et al. 2000, Song et al. 2003, Shkolnik et al. 2009, Schlieder et al. 2010, Murphy et al. 2010, Rodriguez et al. 2011, Riedel et al. 2011, Malo et al. 2013, Rodriguez et al. 2013, Gagné et al. 2014 and subsequent), and thanks to their efforts our samples of low-mass stars to study have been continually growing: we now know of over 650 M-dwarf and lower-mass members of the nearby young moving groups, identified by spectroscopic signs of low surface gravity, age-related lithium absorption, and kinematic matches to the groups.

The question remains, however: given the success of these programs at identifying NYMG members, how many more remain to be discovered? The RECONS[1] TINY proper MOtions (TINYMO) survey (Riedel 2012) delivered a number of new moving group members, many already published in Riedel et al. (2014). Given that the survey has already yielded 26 young stars out of the 55 that have been followed up with astrometry, it is reasonable to assume that the survey may contain many other young stars.

The TINYMO survey contains proper motions measured from the SuperCOSMOS Sky Survey (Hambly et al. 2001b), but these are not sufficient to identify new nearby young stars. A study of moving group identification codes (Riedel et al. submitted) demonstrates that it is impossible to be certain about memberships in a moving group based on proper motions alone; the addition of either radial velocity or parallax measurements (preferably both) dramatically increases the quality of kinematic membership assignments.

Even so, kinematic memberships are only part of the puzzle: motion, no matter how well matched to the moving group's space velocity, is no guarantee the object is actually a young star of the appropriate age. Spectroscopic evidence of youth in the form of measurable lithium or low surface gravity features (weak lines of neutral potassium, sodium, and calcium, Schlieder et al. 2012) are important independent measurements of youth apart from the motion assessment.

Using the South African Large Telescope (SALT), we set out to obtain evidence for stellar youth from radial velocities and spectroscopic parameters for an additional sample of stars from the TINYMO survey. In Section 2, we describe the sample selection process. In Section 3 we detail the observational setup of the Red Side Spectrograph, our observational campaign, and our data reduction procedures. In Section 4, we describe the spectroscopic measurements used to determine the radial velocities and gravity- and activity-sensitive spectral line measurements examined in Section 5, and we discuss the individual young stars in more detail in Section 6.

2. SAMPLE

The sample of stars were drawn from the TINYMO survey (Riedel 2012). In that survey, nearby low-proper-motion M dwarfs in the southern hemisphere were identified in the SuperCOSMOS Science Archive (Hambly et al. 2001b). To be sensitive to stars with proper motions less than $0.18''\mathrm{yr}^{-1}$ all the way down to objects with zero proper motion, an SQL query extracted stars using an *upper* limit on their motion between the photographic plates. Photometric distance relations calibrated to the SuperCOSMOS plate photometry (Hambly et al. 2004) were used to identify stars within 25 parsecs.

The excess luminosity of giant stars makes them appear much closer than they actually are, so a color-color cut was constructed using v^2-K^3 vs. $J-K$ color to filter out giants. This exploits a property of the $J-K$ color, in that when it is plotted against $V-K$ (or any other optical band - K), the locus of giant stars separates from main sequence dwarfs over the approximate spectral type range M1-M6 (Riedel 2012). Consequently, most of the stars in the survey and this paper are of those spectral types, and most of the targets (though not all) have SuperCOSMOS proper motions less than $0.18''\mathrm{yr}^{-1}$. Further searches of catalogs like the General Catalog of Variable Stars (Samus et al. 2012) and Catalog of Galactic Carbon Stars (Alksnis et al. 2001), low-resolution red optical spectroscopy collected at the Lowell Observatory 1.8m and CTIO 1.5m, and quality cuts on the photometric distance estimates reduced the sample of stars potentially within 25 parsecs to 651 objects.

As noted in Riedel (2012), these selection criteria biased the sample toward detecting young stars for two major reasons. First, the space velocities of the nearby young moving groups are clustered around the local standard of rest and thus

arr@caltech.edu

[1] Research Consortium On Nearby Stars, http://www.recons.org

[2] The average of the SuperCOSMOS B_J and second epoch R filter is used as a surrogate V magnitude.

[3] Throughout this paper, K is the 2MASS K_s filter

their members fall within the proper motion selection criteria. Second, young M dwarfs are overluminous, which means that the photometric distance relations identify them as being closer than they really are, and they preferentially scatter into the 25 parsec sample.

In Riedel (2012) and the subsequent work outlined in Riedel et al. (2014), trigonometric parallaxes and spectroscopy were obtained for a subset of identified low-proper-motion M dwarfs whose photometric distances were estimated to place them within 15 parsecs of the Sun, with preference to stars exhibiting X-ray emission (from the ROSAT All-Sky Survey) as a sign of coronal activity.

In this paper, we present red optical spectroscopic observations of 79 stars from the TINYMO survey selection of 651 potential nearby M dwarfs regardless of activity level. The targets are bright M dwarfs published in Riedel et al. (2014) without radial velocities (as of 2013 when observations took place; several radial velocities were published afterwards), and TINYMO M dwarfs that have not been studied before. Targets were prioritized by their SuperCOSMOS plate I_{59} magnitudes. They cover a photographic plate magnitude range of I_{59}=9.12 (NLTT 47004AB) to I_{59}=10.85 (SCR 1316-0858). As these are the brightest targets, this sample is expected to be biased toward closer stars, binaries, and extremely young stars. Together with Riedel et al. (2014), 100 stars from the TINYMO sample have been followed up.

We have chosen to replace the astrometry and photometry from the Hambly et al. (2001b) SuperCOSMOS catalog with more recent and precise CCD-based measurements. SuperCOSMOS's astrometry is relative, not absolute, and contains proper motions forced to zero average on a per-photographic-field basis, which we have replaced with absolute ICRS-grid positions and proper motions from UCAC4 (Zacharias et al. 2013) or PPMXL (Roeser et al. 2010) where UCAC4 motions were not available. SuperCOSMOS's photometry, though internally consistent, is photographic plate measurements in blue, red, and infrared (Hambly et al. 2001a); we have instead elected to use Johnson V CCD photometry from the AAVSO Photometric All Sky Survey (APASS) Data Release 9 (Henden et al. 2016), and K near-infrared photometry from the Two Micron All Sky Survey (2MASS, Cutri et al. 2003). The adopted literature data are collected in Table 1.

Table 1. Previously Published Astrometry and Photometry

Name	RA	DEC	pos.	μ_{RA}[a]	μ_{DEC}	μ	π		V		K	
	(J2000 E2000)		ref.	($''yr^{-1}$)		ref.	(mas)	ref.	(mag.)	ref.	(mag.)	ref.
SCR 0017-6645	004.348112	-66.753424	1	102.9± 1.0	-15.0± 1.0	1	25.61±1.73	3	12.49±0.04	7	7.70±0.02	1
GJ 2006A	006.959305	-32.551783	1	99.2± 1.3	-61.3± 2.6	1	30.97±1.76	3	12.82±0.06	7	8.01±0.03	1
GJ 2006B	006.959810	-32.556723	1	117.2± 4.1	-31.5± 5.8	1	30.97±1.76	3	13.14±0.04	7	8.12±0.03	1
HIP 3556	011.367317	-51.626090	1	100.3± 1.3	-57.1± 0.9	1	24.78±2.65	4	11.97±0.04	7	7.62±0.03	1
SCR 0106-6346	016.594516	-63.777545	1	150.3± 1.3	65.0± 1.3	1			13.40±0.04	7	8.39±0.03	1
[PS78] 190	020.683483	-25.785484	1	50.3± 1.1	6.1± 1.5	1			13.01±0.05	7	8.28±0.03	1
BAR 161-12	023.808013	-07.214303	1	93.0± 1.7	-48.0± 2.2	1	33.70±0.26	5	13.43±0.04	7	8.08±0.03	1
GIC 138	023.985392	-13.429697	1	119.5± 2.5	-21.5± 3.2	1			13.36±0.01	7	8.81±0.02	1
L 173-39	027.108869	-56.978227	1	255.6± 8.0	-35.0± 8.0	1			11.72±0.02	7	7.32±0.02	1
SCR 0149-5411	027.274579	-54.199205	1	120.0± 1.4	-18.0± 1.4	1			13.15±0.02	7	8.85±0.02	1
SCR 0152-5950	028.076259	-59.837995	1	109.2± 1.8	-25.7± 1.8	1			12.49±0.08	7	8.14±0.03	1
SCR 0212-5851	033.242464	-58.855051	1	87.7± 1.3	-15.9± 1.3	1			12.92±0.03	7	8.44±0.02	1
SCR 0213-4654	033.375897	-46.914036	1	42.5± 1.0	4.9± 1.0	1			13.78±0.07	7	8.60±0.02	1
SCR 0215-0929	033.995595	-09.486749	1	96.6± 1.9	-46.5± 2.6	1			12.21±0.05	7	7.55±0.02	1
SCR 0220-5823	035.214147	-58.394755	1	97.3± 2.0	-13.0± 2.0	1			13.92±0.01	7	8.83±0.02	1
SCR 0222-6022	035.683964	-60.379890	1	137.4± 1.7	-13.8± 1.7	1			13.33±0.05	7	8.10±0.03	1
2MASS 0236-5203	039.215438	-52.051011	1	102.2± 0.8	1.2± 0.8	1			12.05±0.09	7	7.50±0.03	1
LP 886-73	039.823509	-26.821910	1	98.7± 2.9	-40.2± 1.3	1			14.33±0.05	7	8.75±0.02	1
SCR 0248-3404	042.219172	-34.073538	1	90.2± 1.4	-23.7± 1.4	1			13.64±0.02	7	8.40±0.03	1
SCR 0254-5746	043.526282	-57.776673	1	102.9± 1.1	7.2± 1.2	1			13.37±0.03	7	8.83±0.02	1
2MASS 0254-5108A	043.638184	-51.142059	1	92.0± 1.2	-11.9± 1.2	1			12.07±0.03	7	7.79±0.03	1
SCR 0256-6343	044.196132	-63.717440	1	67.4± 2.2	8.3± 5.6	1			14.23	8	9.01±0.03	1
LP 831-35	047.512712	-23.691887	1	98.3± 1.3	-134.8± 1.3	1			13.49±0.04	7	8.57±0.03	1
2MASS 0510-2340A	077.517787	-23.678016	1	41.4± 2.3	-13.3± 1.1	1			13.04±0.03	7	8.36±0.02	1
2MASS 0510-2340B	077.520402	-23.670874	1	34.8± 2.7	-13.8± 1.5	1			13.29±0.05	7	8.54±0.02	1
SCR 0522-0606	080.669559	-06.106641	1	17.0± 3.2	-21.1± 3.3	1			14.27±0.06	7	9.13±0.02	1

Table 1 continued

Table 1 *(continued)*

Name	RA	DEC	pos.	μ_{RA}[a]	μ_{DEC}	μ	π		V		K	
	(J2000 E2000)		ref.	($''yr^{-1}$)		ref.	(mas)	ref.	(mag.)	ref.	(mag.)	ref.
SCR 0711-3510AB	107.996535	-35.171050	1	-27.7± 1.2	-57.9± 1.6	1			13.65±0.06	7	8.79±0.02	1
SCR 0844-0637	131.231937	-06.623875	2	-58.3± 5.3	-126.4± 5.3	2			13.38±0.05	7	8.51±0.02	1
LP 728-71	148.174075	-15.603822	1	-117.0± 1.2	-135.2± 1.3	1			13.46±0.05	7	8.51±0.02	1
SCR 1012-3124AB	153.037878	-31.412579	1	-74.8± 1.1	-9.4± 1.0	1	18.54±1.74	3	13.42±0.07	7	7.99±0.03	1
TWA 3ABCD	167.616225	-37.531102	1	-105.9± 0.9	-17.3± 1.0	1			12.05±0.01	7	6.77±0.02	1
SCR 1121-3845	170.272849	-38.754586	1	-66.6± 1.5	-11.7± 1.5	1	15.59±0.70	6	12.59±0.06	7	8.05±0.03	1
TWA 5ABC	172.980251	-34.607570	1	-79.6± 0.8	-22.6± 0.9	1	19.97±0.70	6	11.45±0.13	7	6.75±0.02	1
RX 1132-3019	173.076313	-30.331070	1	-87.8± 1.3	-25.2± 1.3	1			14.41	8	8.77±0.02	1
RX 1132-2651A	173.171855	-26.865554	2	-99.2± 6.2	-32.2± 6.2	2	21.28±1.01	3	12.27±0.02	7	7.43±0.02	1
SIPS 1145-4055	176.398474	-40.932576	1	-277.2± 8.0	-131.9± 8.0	1			14.22±0.04	1	8.79±0.02	1
LP 851-410	179.582406	-22.683258	1	-105.1± 1.9	-65.1± 1.0	1			13.20±0.05	7	8.43±0.02	1
SCR 1200-1731	180.006620	-17.525233	1	-81.0± 1.1	-24.6± 1.2	1			13.83±0.06	7	8.47±0.03	1
2MASS 1207-3247	181.864072	-32.783402	1	-70.4± 1.4	-29.7± 1.1	1	18.55±0.48	6	12.64±0.04	7	7.75±0.03	1
L 758-107	182.820600	-19.972708	1	-204.5± 2.1	-190.6± 3.0	1			12.62±0.02	7	7.74±0.02	1
SCR 1230-3300	187.720947	-33.014119	1	-156.7± 0.8	0.0± 0.8	1			12.56±0.03	7	8.09±0.02	1
SCR 1233-3641	188.380858	-36.694691	1	-55.8± 0.9	-49.9± 0.9	1			13.44±0.03	7	8.74±0.02	1
SCR 1237-4021	189.301605	-40.363386	1	-63.7± 1.1	-29.1± 1.1	1			13.50±0.06	7	8.52±0.02	1
SCR 1238-2703	189.654646	-27.059737	2	-185.1± 5.1	-185.2± 5.1	2			12.44±0.03	7	7.84±0.03	1
SCR 1316-0858	199.168930	-08.973762	1	-57.5± 4.2	-56.2± 7.7	1			14.57±0.06	7	9.20±0.02	1
SCR 1321-1052	200.484680	-10.869421	1	-66.6± 3.1	-50.5± 3.8	1			13.90±0.03	7	8.62±0.02	1
SCR 1421-0916	215.359374	-09.282748	1	-135.3± 3.3	-18.5± 1.2	1			13.73±0.07	7	8.94±0.02	1
SCR 1421-0755	215.391939	-07.921291	1	-95.1± 2.2	-86.4± 1.2	1			13.61±0.01	7	8.63±0.02	1
SCR 1425-4113AB	216.371348	-41.225645	1	-46.8± 2.1	-49.2± 1.7	1	14.94±0.96	3	12.62±0.05	7	7.61±0.02	1
SCR 1438-3941	219.651047	-39.685075	1	-109.8± 1.0	-104.5± 2.2	1			12.73±0.01	7	8.52±0.02	1
LP 914-6	220.092260	-27.878378	1	-127.9± 8.0	-202.2± 8.0	1			13.62±0.01	7	8.75±0.02	1
SCR 1521-2514	230.461609	-25.236576	1	-32.4± 1.4	-56.2± 2.0	1			13.38±0.03	7	8.65±0.02	1
SCR 1708-6936	257.036730	-69.605169	1	-54.6± 1.7	-81.1± 1.7	1			13.16±0.02	7	8.20±0.02	1
SCR 1816-6305	274.211919	-63.088775	1	-117.5± 6.1	-47.3± 2.0	1			12.74±0.01	7	8.39±0.03	1
SCR 1842-5554A	280.528984	-55.907110	1	9.7±12.1	-81.2± 2.8	1			13.59±0.14	7	8.58±0.02	1
NLTT 47004AB	282.172344	-46.785495	2	196.6± 3.2	125.6± 3.2	2			11.60±0.02	7	6.99±0.04	1
SCR 1856-6922	284.018227	-69.366773	1	-10.8± 1.4	-115.6± 2.3	1			12.44±0.04	7	7.70±0.02	1
WT 625	286.334771	-54.578257	1	86.2± 8.0	-213.3± 8.0	1			13.34±0.01	1	8.55±0.02	1
SCR 1922-6310	290.711309	-63.182795	1	-7.9±16.7	-77.5± 1.9	1			13.31±0.06	7	8.58±0.02	1
RX 1924-3442	291.145631	-34.710924	1	22.1± 1.8	-71.7± 1.8	1			14.24±0.06	7	8.79±0.03	1
SCR 1926-5331	291.503116	-53.524166	1	34.1± 2.1	-87.4± 2.1	1			14.03±0.13	7	8.68±0.02	1
SCR 1938-2416	294.653739	-24.282940	1	33.5± 1.8	67.6± 5.8	1			13.10±0.03	7	8.51±0.02	1
SCR 1951-4025	297.899813	-40.422480	2	40.8±14.0	-186.1±14.0	2			13.55±0.02	7	8.71±0.02	1
SCR 2004-6725A	301.038323	-67.419721	1	7.0± 1.3	-84.5± 2.4	1			13.11±0.02	7	8.48±0.02	1
2MASS 2004-3356	301.118608	-33.936334	1	69.4± 2.5	-103.3± 2.6	1			14.61±0.05	7	9.17±0.02	1
SCR 2008-3519	302.223697	-35.330161	1	49.4± 1.3	-76.7± 1.3	1			13.52±0.06	7	8.32±0.03	1
SCR 2010-2801AB	302.500154	-28.028066	1	40.7± 3.0	-62.0± 1.7	1	20.85±1.33	3	12.98±0.02	7	7.73±0.03	1
L 755-19	307.181835	-11.475196	2	166.4± 5.2	-93.3± 5.2	2	53.18±1.67	3	12.52±0.04	7	7.50±0.03	1
SCR 2107-7056	316.843702	-70.936854	1	27.5± 1.5	-91.6± 1.4	1			13.86±0.08	7	8.90±0.02	1
SCR 2107-1304	316.903307	-13.082831	1	59.4± 1.3	-86.0± 3.0	1			12.64±0.08	7	7.84±0.03	1
LEHPM 1-4147	323.717454	-63.018961	2	105.9±14.0	-134.9±14.0	2			13.47±0.04	7	8.74±0.03	1
SCR 2204-0711	331.165971	-07.192684	1	-3.1± 1.3	-4.2± 1.4	1			12.27±0.21	7	-8.49±0.02	1

Table 1 continued

Table 1 *(continued)*

Name	RA	DEC	pos.	μ_{RA}[a]	μ_{DEC}	μ	π		V		K	
	(J2000 E2000)		ref.	($''yr^{-1}$)		ref.	(mas)	ref.	(mag.)	ref.	(mag.)	ref.
SCR 2237-2622	339.312287	-26.375884	1	145.4± 1.5	-11.8± 1.5	1			13.33±0.04	7	8.31±0.02	1
SIPS 2258-1104	344.568493	-11.071400	1	106.8± 2.9	-5.9± 2.9	1			12.97±0.05	7	8.24±0.03	1
LEHPM 1-5404	345.456139	-53.285470	2	151.1±16.1	-234.0±16.1	2			13.11±0.04	7	8.50±0.02	1
SCR 2328-6802	352.240163	-68.042788	1	66.8± 1.9	-67.1± 1.7	1			13.02±0.04	7	8.38±0.02	1
LTT 9582	353.000790	-39.293587	2	193.4±17.9	-178.4±17.9	2			12.96±0.07	7	8.02±0.02	1
G 275-71	353.953102	-24.319238	1	106.5± 1.1	-120.7± 1.0	1			13.71±0.02	7	8.77±0.02	1
LEHPM 1-6053	355.099384	-40.363084	2	262.5±13.3	-131.0±13.3	2			12.94±0.02	7	8.34±0.03	1

NOTE—The kinematic data used by LACEwING (in section 5) and photometric data used in our youth analysis. Literature RVs were not used even wh exist. 1.) UCAC4 (includes APASS DR6 $g'r'i'BV$ and 2MASS JHK_s) Zacharias et al. (2013), 2.) PPMXL Roeser et al. (2010), 3.) Riedel et al. (20 van Leeuwen (2007), 5.) Shkolnik et al. (2012), 6.) Weinberger et al. (2013), 7.) Henden et al. (2016) 8.) Zacharias et al. (2005). *The online machine-r version of this table is a merged table including Table 2, Table 5, and Table 6.*

[a] μ_{RA} is actually $\mu_{RA\cos DEC}$ everywhere it appears.

3. OBSERVATIONS

The South African Large Telescope (SALT) is an 11-meter telescope hosted at the South African Astronomical Observatory (SAAO) in Sutherland, South Africa. It is based on the design of the McDonald Observatory Hobby-Eberly Telescope (Buckley et al. 2006) and shares the segmented mirror and fixed-altitude design of that telescope, yielding an effective mirror diameter of 9.2 meters. The large collecting area and advantageous position in the southern hemisphere (where most of the NYMGs are concentrated) make SALT an efficient and effective means of collecting high SNR low resolution spectra of young M dwarfs even under bad weather conditions. It was thus possible to schedule usable observations at all times despite SALT's fixed altitude and the associated maximum tracking time requirements for objects at mid-southern declinations.

We have obtained low resolution optical spectroscopy from the SALT telescope and the Robert Stoble Spectrograph (RSS, Kobulnicky et al. 2003), which provides optical spectroscopy between 3200-9000Å with a resolving power of up to 6000, depending on slit width.

Observations were conducted in semesters 2013A and 2013B, utilizing bad-weather time; on many occasions only a single star was observed each night. At all times, the PG1800 filter was used with a 1″ slit and the PC04600 grating at an angle of 40.25 degrees. In this mode, RSS delivers spectra covering 6500-7800Å with a resolving power of R=5000, covering the Hα 6563Å line, the Lithium 6708Å doublet, and the Potassium 7699Å line. The RSS chip is split into 3 equal segments, which can be reduced separately; in this way, the chips cover roughly 6500-6900Å, 6950-7350Å, and 7400-7800Å. During the 2013A semester, a Neon arc lamp was used; in 2013B, this was changed to Xenon to obtain more evenly spaced lines.

Two spectra were taken per visit in a 2x2 binning mode with slow readout and with exposure times calculated for 5″ seeing conditions (in practice, the seeing was never that bad). With these conditions and bright targets (exposures were never longer than 620 seconds), signal to noise ratios of over 100 were generally reached.

In total, there are 165 spectra of the 79 stars: SCR 2237-2622 was only observed once; two stars (SCR 1816-6305, 2MASS 2004-3356) were observed three times, three stars (2MASS 0510-2340B, 2MASS 1207-3247, SCR 1842-5554A) were observed four times, and the remainder were observed twice. Twelve spectra of telluric standard stars were also taken. The entire observing program totaled 140,000 seconds (39 hours) of observing time.

Data were reduced with PyRAF and the Astropy astronomical python package (Astropy Collaboration et al. 2013), using standard IRAF long-slit reduction techniques. The individual RSS chips were treated separately, to increase the accuracy of radial velocity calibrations. The wavelength calibration error obtained by IRAF was around 0.04Å for both Xenon and Neon arc lamps. Of all the flux standards observed, only Hiltner 600, observed in 2013B, was taken with sufficient signal to noise to be used in reductions.

4. ANALYSIS

Spectral types (Table 2) were determined using the MATCHSTAR code (Riedel et al. 2014), an automated template matching code which compares red optical spectra to RECONS K and M standard star spectra (Kirkpatrick et al. 1991; Henry et al. 1994, 2002) between 6000Å-9000Å, after trimming and degrading resolution so that input and standard spectra overlap. With the prioritization of the brightest M dwarfs in the sample, it is unsurprising that most of the objects skew toward the hotter M dwarfs - M1.0V-M3.0V. The hottest star is SCR 2204-0711, K9.0Ve (though see Section 6.9); the coolest star is RX 1132-3019, M4.5Ve (Figure 1). Spectral types are given in Table 2.

4.1. *Radial velocities*

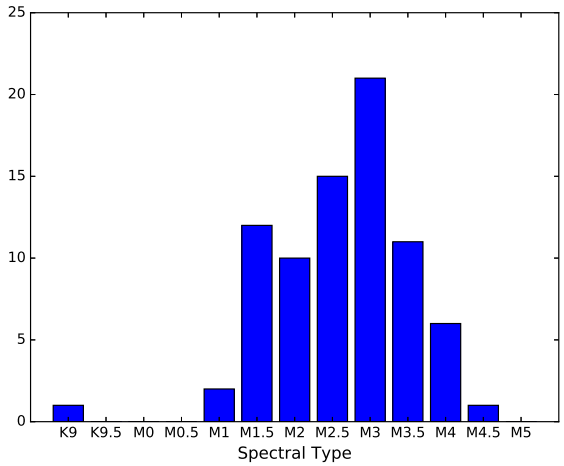

Figure 1. Distribution of spectral types of objects in the sample.

Radial velocities (RVs) were measured from the SALT data using the same code developed for and used in Faherty et al. (2016). The code cross-correlates the spectrum of a star of unknown RV, to one of known RV and the same spectral type. The process is repeated 1000 times, adding random Gaussian noise scaled to the per-pixel flux uncertainties of both the known and unknown star's spectrum, in order to quantify the effect of noise on the radial velocity measurement. The RV results of the 1000 iterations are then binned into a histogram and fit with a Gaussian to determine the mean radial velocity and uncertainty.

As noted in Faherty et al. (2016), this cross-correlation technique still under-estimates the true uncertainties in the measured RV. To accommodate systematic errors in the data, we cross-correlate the spectra against multiple comparison stars and combine the results with a weighted standard deviation. Ideally, the comparison stars would be RV standards, but we did not observe any radial velocity standards. Instead, we selected thirteen stars with previously measured RVs with uncertainties less than 2 km s^{-1} for use as velocity comparisons. We measured the RVs of the comparison stars relative to each other other (the stars marked "C" in Table 2) to demonstrate the accuracy and precision of the radial velocities.

Six spectral regions were considered for RV measurement (Figure 2). (1) The first chip, in a 50Å region surrounding the Hα line (6530-6580Å), (2) the first chip, truncated at the atmospheric B band (6500-6840Å), (3) the first chip, with both the Hα and atmospheric B band removed (6570-6840Å), (4) the second chip, covering 6980-7350Å, (5) the third chip, blueward of the atmospheric A band (7400-7580Å), and (6), the third chip, redward of the atmospheric A band. (7680-7720Å). Initial RV measurements showed the original wavelength calibrations to both the neon and xenon lamps were insufficient for RV work. RVs of our comparison stars were typically discrepant from published values by over 10 km s^{-1}, even after being combined in weighted standard deviations.

We investigated the possibility of improving our precision by using the atmospheric A and B bands (regions shown in Figure 2) to correct the wavelength solution. The first procedure attempted involved independently cross-correlating chip 1 and chip 3 to an atmospheric template spectrum (Hinkle et al. 2003) to obtain zero-point corrections to the wavelength solution, before applying the heliocentric correction. This initial procedure produced a significant improvement in accuracy, but prevented the use of chip 2, which lacks prominent atmospheric features. A further improvement was made using the centers of the A and B bands to derive a linear correction as a function of input wavelength. This produced significantly better accuracy than the zero point correction, and it was found that the best results came from the second chip (region 4), where precisions of 3-6 km s^{-1} have been achieved. All RV results in Table 2 derive from spectral region 4 with the two-point linear wavelength correction.

While it is known that spectral type matches are important to obtain precise RVs, all of our targets have very similar spectral types, and our precision appears to be low enough that those spectral morphological differences do not affect our results. Instead, we found three stars – SCR 0017-6645, SCR 0152-5950, and 2MASS 1207-3247 – that produced uniformly low accuracy and low precision results in every cross-correlation. These were removed from consideration, and the radial velocity results are based on the weighted mean and weighted standard deviation of the other 10 stars with known RVs. The RV results and uncertainties in Table 2 are thus the weighted standard deviation of between 10 and 40 measurements, depending on the number of spectra for the target. Of the 34 total stars in the sample with existing radial velocity measurements, 24 of our measurements (70%) are within 1-σ of those reported errors and 29 (85%) are within 2-σ. Given the small number of RV crossmatches, we believe this demonstrates the accuracy of our RVs despite our relatively low precision.

Table 2. Radial Velocities and Spectral Types

C[a]	Name	RA (J2000)	DEC (J2000)	Spectral Type	R.V. (km s^{-1})	Literature R.V. (km s^{-1})	ref.
X	SCR 0017-6645	00 17 23.52	-66 45 12.5	M3.0 Ve	-4.8 ± 5.6	$+11.4\pm0.8$	1
	GJ 2006A	00 27 50.24	-32 33 06.1	M3.5 Ve	-24.9 ± 4.6		

Table 2 continued

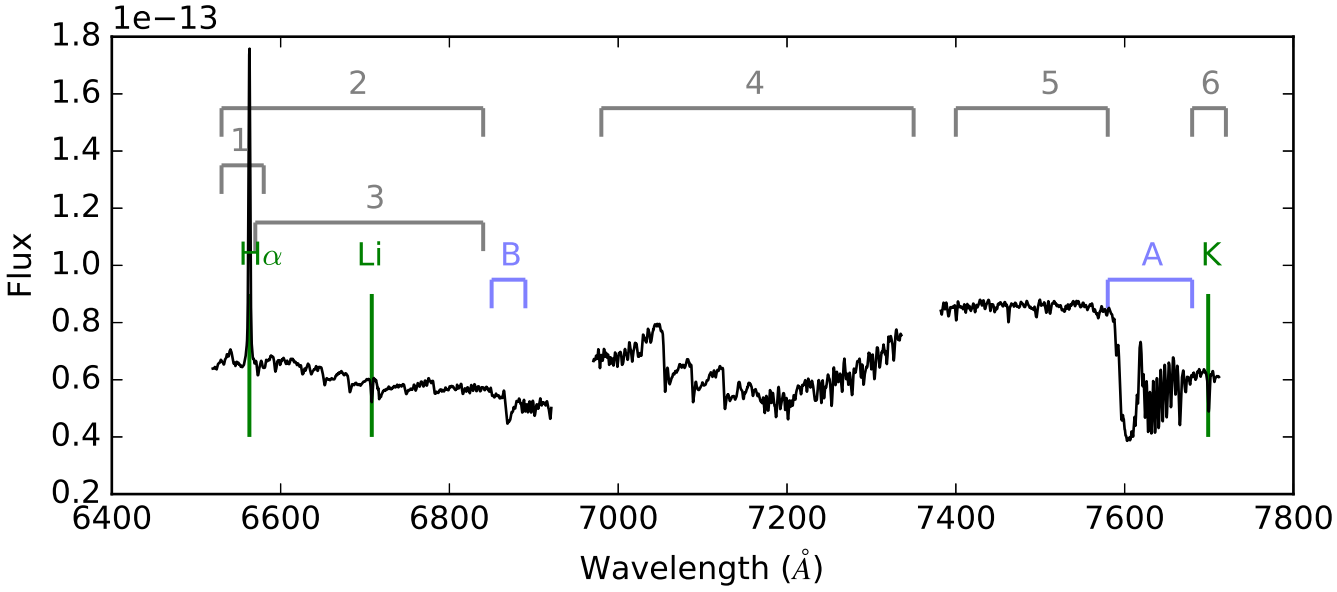

Figure 2. Spectrum of RXJ 1132-2651A (TWA 8A) showing the spectral regions considered for RV fits, the spectral lines measured, and the regions used for the telluric correction to the atmospheric A and B bands.

Table 2 *(continued)*

C[a]	Name	RA (J2000)	DEC (J2000)	Spectral Type	R.V. (km s^{-1})	Literature R.V. (km s^{-1})	ref.
	GJ 2006B	00 27 50.36	-32 33 23.9	M3.5 Ve	+6.9±6.1		
	HIP 003556	00 45 28.15	-51 37 34.0	M1.5 Ve	−0.7±4.9	−1.6±20	1
	SCR 0106-6346	01 06 22.67	-63 46 39.1	M3.0 Ve	+13.3±5.2		
	[PS78] 190	01 22 44.04	-25 47 07.8	M3.0 Ve	+3.6±5.4		
	BAR 161-12	01 35 13.94	-07 12 51.8	M4.0 Ve	+19.0±5.8	+11.7±5.3	2
	GIC 138	01 35 56.45	-13 25 47.3	M1.5 Ve	−26.4±7.2		
	L 173-39	01 48 26.17	-56 58 41.5	M1.5 Ve	+33.6±5.5		
	SCR 0149-5411	01 49 05.92	-54 11 57.2	M1.0 Ve	+2.1±4.1		
X	SCR 0152-5950	01 52 18.31	-59 50 16.8	M2.0 Ve	+14.0±5.3	+7.9±1.6	1
	SCR 0212-5851	02 12 58.20	-58 51 18.2	M2.0 Ve	+4.5±5.0	+9.1±0.8	3
	SCR 0213-4654	02 13 30.22	-46 54 50.5	M3.0 Ve	+9.4±6.0	+14.3±2.0	4
	SCR 0215-0929	02 15 58.93	-09 29 12.2	M2.5 Ve	+15.4±5.5	+10.1±0.6	3
	SCR 0220-5823	02 20 51.39	-58 23 41.1	M3.5 Ve	+18.3±6.3	+12.1±0.6	3
	SCR 0222-6022	02 22 44.17	-60 22 47.6	M3.5 Ve	+28.6±7.0	+16.2±1.5	3
C	2MASS 0236-5203	02 36 51.71	-52 03 03.7	M2.0 Ve	+12.9±5.5	+16.0±0.1	5
	LP 886-73	02 39 17.64	-26 49 18.9	M4.0 Ve	−16.5±6.4		
C	SCR 0248-3404	02 48 52.62	-34 04 24.7	M3.5 Ve	+14.5±5.5	+14.6±0.3	4
	SCR 0254-5746	02 54 06.31	-57 46 36.1	M2.5 V	+0.1±5.0		
	2MASS 0254-5108A	02 54 33.17	-51 08 31.4	M1.5 Ve	+13.0±5.1	+13.8±0.4	3
	SCR 0256-6343	02 56 47.09	-63 43 02.8	M4.0 Ve	−10.9±6.0	+16.2±3.4	4
	LP 831-35	03 10 03.07	-23 41 31.0	M3.5 Ve	+25.5±6.1		
	2MASS 0510-2340A	05 10 04.27	-23 40 40.7	M3.0 Ve	+18.8±5.2	+24.2±0.2	4
	2MASS 0510-2340B	05 10 04.88	-23 40 14.9	M2.5 Ve	+15.6±7.5	+23.8±0.5	4
	SCR 0522-0606	05 22 40.70	-06 06 23.9	M2.5 Ve	−1.5±5.0		
	SCR 0711-3510AB	07 11 59.17	-35 10 15.7	M3.0 Ve	+4.1±5.0		

Table 2 continued

Table 2 *(continued)*

C[a]	Name	RA (J2000)	DEC (J2000)	Spectral Type	R.V. (km s^{-1})	Literature R.V. (km s^{-1})	ref.
	SCR 0844-0637	08 44 55.66	-06 37 26.0	M2.0 Ve	−18.0±2.0		
	LP 728-71	09 52 41.77	-15 36 13.7	M2.5 V	−5.6±3.4		
	SCR 1012-3124AB	10 12 09.08	-31 24 45.2	M3.5 Ve	+14.6±5.5	+14.69±0.53	6
C	TWA 3ABCD	11 10 27.88	-37 31 52.0	M3.5 Ve	+14.5±2.5	+15.6±0.2	5
C	SCR 1121-3845	11 21 05.49	-38 45 16.4	M1.0 Ve	+9.5±2.2	+12.7±1.0	5
	TWA 5ABC	11 31 55.26	-34 36 27.3	M1.5 Ve	+10.2±2.2	+12.7±3.8	5
C	RX 1132-3019	11 32 18.31	-30 19 51.8	M4.5 Ve	+15.8±4.7	+12.3±1.5	7
C	RX 1132-2651A	11 32 41.25	-26 51 55.9	M2.0 Ve	+7.8±2.5	+8.68±0.02	1
	SIPS 1145-4055	11 45 35.70	-40 55 57.0	M2.5 Ve	+14.2±6.2		
	LP 851-410	11 58 19.78	-22 40 59.7	M2.5 Ve	−36.7±4.3		
	SCR 1200-1731	12 00 01.60	-17 31 30.8	M3.5 Ve	+20.1±2.4		
X	2MASS 1207-3247	12 07 27.38	-32 47 00.3	M2.5 Ve	−16.4±2.9	+8.5±1.2	8
C	L 758-107	12 11 16.95	-19 58 21.7	M2.5 V	−12.0±4.9	−9.226±0.1	9
	SCR 1230-3300	12 30 53.02	-33 00 50.8	M1.5 Ve	+20.7±2.2		
	SCR 1233-3641	12 33 31.40	-36 41 40.8	M2.0 Ve	+6.7±4.4		
	SCR 1237-4021	12 37 12.38	-40 21 48.1	M2.5 Ve	+11.3±2.4		
	SCR 1238-2703	12 38 37.13	-27 03 35.0	M1.5 Ve	+0.5±3.3	+9.9±0.2	4
	SCR 1316-0858	13 16 40.54	-08 58 25.6	M3.0 Ve	+6.1±4.9		
	SCR 1321-1052	13 21 56.31	-10 52 09.9	M3.5 Ve	+26.5±5.6	−4.2±2.2	4
	SCR 1421-0916	14 21 26.24	-09 16 58.0	M2.0 V	−4.3±4.3		
	SCR 1421-0755	14 21 34.06	-07 55 16.6	M3.0 V	−5.2±7.2		
	SCR 1425-4113AB	14 25 29.20	-41 13 32.0	M3.0 Ve	+12.4±3.7		
	SCR 1438-3941	14 38 36.40	-39 41 04.0	M1.5 V	+36.6±5.9		
	LP 914-6	14 40 22.30	-27 52 39.0	M3.0 Ve	+17.5±4.1		
	SCR 1521-2514	15 21 50.80	-25 14 11.0	M1.5 Ve	−0.8±2.9		
	SCR 1708-6936	17 08 09.00	-69 36 18.0	M3.0 Ve	+11.3±3.4	+9.4±3.5	4
	SCR 1816-6305	18 16 51.10	-63 05 19.0	M1.5 V	+33.5±0.9		
	SCR 1842-5554A	18 42 06.95	-55 54 25.5	M3.0 Ve	+9.8±4.9	+0.3±0.5	4
	NLTT 47004AB	18 48 41.10	-46 47 10.0	M2.5 Ve	+21.0±4.0		
	SCR 1856-6922	18 56 04.40	-69 21 59.0	M3.0 V	+21.1±4.0		
	WT 625	19 05 20.20	-54 34 40.0	M3.0 Ve	−15.6±4.3		
	SCR 1922-6310	19 22 50.70	-63 10 57.0	M3.0 Ve	+5.7±2.1	+6.5±1.6	4
C	RX 1924-3442	19 24 34.95	-34 42 39.4	M4.0 Ve	−7.7±5.7	−3.7±0.2	4
	SCR 1926-5331	19 26 00.75	-53 31 26.9	M4.0 Ve	−7.6±6.0		
	SCR 1938-2416	19 38 36.90	-24 17 00.0	M2.0 Ve	+14.4±3.9		
	SCR 1951-4025	19 51 35.90	-40 25 18.0	M1.5 Ve	+20.6±5.9		
	SCR 2004-6725A	20 04 09.20	-67 25 09.0	M2.5 Ve	+10.4±3.5		
	2MASS 2004-3356	20 04 28.47	-33 56 10.7	M4.0 Ve	−16.1±3.8		
	SCR 2008-3519	20 08 53.60	-35 19 47.0	M3.0 Ve	−5.9±6.3		
	SCR 2010-2801AB	20 10 00.03	-28 01 41.2	M3.0 Ve	+1.0±4.2	−5.8±0.6	4
	L 755-19	20 28 43.40	-11 28 29.0	M1.5 Ve	−31.2±5.8		
	SCR 2107-7056	21 07 22.48	-70 56 12.6	M3.0 Ve	+3.3±4.6		
	SCR 2107-1304	21 07 36.70	-13 04 56.0	M3.0 Ve	−3.7±4.8	−2.3±0.5	4
	LEHPM 1-4147	21 34 52.00	-63 01 06.0	M2.5 V	+12.4±4.0		
	SCR 2204-0711[b]	22 04 39.83	-07 11 33.7		−204.9±12.1		
	SCR 2237-2622	22 37 14.95	-26 22 33.3	M3.5 Ve	+3.4±5.0		

Table 2 continued

Table 2 *(continued)*

C[a]	Name	RA	DEC	Spectral	R.V.	Literature R.V.	
		(J2000)		Type	(km s^{-1})	(km s^{-1})	ref.
C	SIPS 2258-1104	22 58 16.44	-11 04 17.1	M3.0 Ve	+20.2±5.5	+16.0±0.2	2
	LEHPM 1-5404	23 01 49.48	-53 17 07.7	M2.0 V	+12.3±6.7		
	SCR 2328-6802	23 28 57.64	-68 02 33.9	M2.5 Ve	+3.5±5.1	+8.0±1.5	3
C	LTT 9582	23 32 00.19	-39 17 36.9	M3.0 Ve	+8.7±5.3	+11.6±0.7	1
	G 275-71	23 35 48.75	-24 19 09.3	M2.5 V	−2.9±7.7		
	LEHPM 1-6053	23 40 23.85	-40 21 47.1	M2.0 Ve	+25.2±5.7		

NOTE—Literature RV sources: 1.) Malo et al. (2013), 2.) Shkolnik et al. (2012), 3.) Kraus et al. (2014), 4.) Malo et al. (2014), 5.) Torres et al. (2006), 6.) Riedel et al. (2014), 7.) Looper et al. (2010), 8.) Schneider et al. (2012), 9.) Nidever et al. (2002)

[a] Stars are noted as "C" if their spectra were used as comparisons for the RV fitting, and "X" if they were rejected as comparisons.

[b] Giant, see 6.9

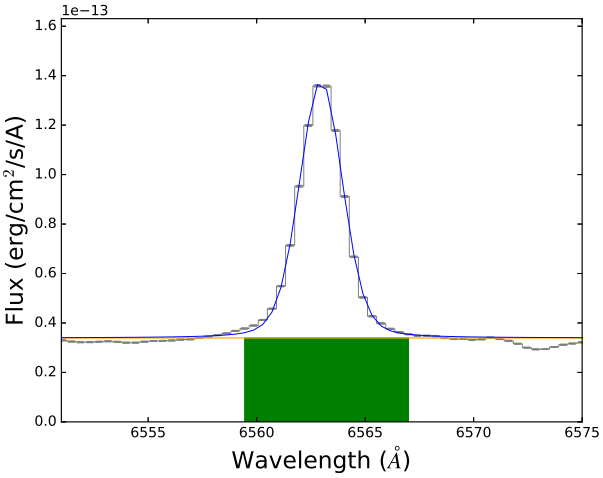

Figure 3. Hα (6563 Å) EW of RX 1132-2651A (TWA 8A), as an example. The pseudocontinuum (yellow) and Voigt profile (blue) are fit to the observed spectrum (grey). The green rectangle approximates the EW.

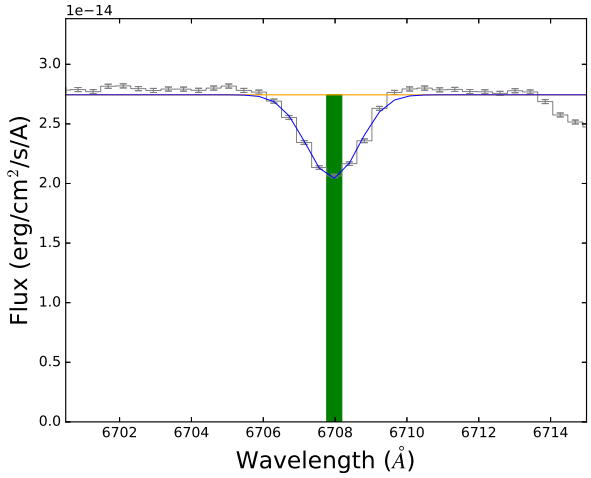

Figure 4. Li (6708 Å) EW of RX 1132-2651A (TWA 8A), as an example. The pseudocontinuum and Voigt profile are shown according to Figure 3. The green rectangle approximates the EW.

4.2. *Spectral Line Measurements*

To evaluate spectroscopic signatures of youth, we measure equivalent widths of the Hα (6563 Å) emission line, the unresolved Li (6708 Å) doublet, and the K I (7699 Å) absorption line for all 177 low-resolution optical spectra taken with SALT. To aid us in these measurements, we employ PHEW: PytHon Equivalent Widths (Alam & Douglas 2016), which is based on the Pythonic spectroscopic line analysis toolkit PySpecKit[4] (Ginsburg & Mirocha 2011).

For each case, we fit a 0th-order baseline to the average flux of the nearby pseudocontinuum, and set the line window to be between 6550-6580 Å (Figure 3), 6700-6715 Å (Figure 4), and 7685-7711 Å (Figure 5) for the Hα, Li, and K I lines, respectively. We then fit a Voigt profile to the spectral line in each window. (For features that do not have well-defined wings at this resolution, equivalent widths were measured with a Gaussian profile fit to the feature.) The equivalent width is then calculated by integrating the pseudocontinuum level minus the spectrum over the selected range. Uncertainties were estimated through Monte Carlo analysis of 500 iterations, for every spectrum. We have combined all measurements for a given star with a weighted mean and standard deviation, which we report in Table 6, and summarize in Table 5. For further information about interesting objects and trends in these line measurements, see Section 6.

[4] http://pyspeckit.bitbucket.org/html/sphinx/index.html

5. RESULTS

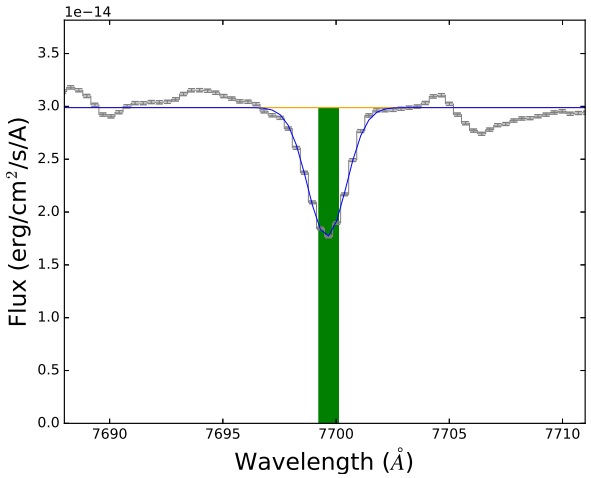

Figure 5. K I (7699 Å) EW of RX 1132-2651A (TWA 8A), as an example. The EW itself is approximated by the green rectangle. A Voigt profile and pseudocontinuum fit are shown as in Figures 3 and 4.

5.1. *Hα (6563Å) activity indicator*

Hα emission, while related to youth, is not a reliable indicator of youth for M dwarfs as their activity can persist for billions of years. As shown by West et al. (2008), M0-M2 stars with Hα emission are typically younger than 1 Gyr; M3 stars are generally less than 2 Gyr old, suggesting most of our stars are younger than field age. Checking the T Tauri veiling limit in Hα EW from White & Basri (2003) suggests that none of the stars in this sample are potential T Tauri stars, which should be expected from the relative rarity of such objects within 100 parsecs, although RX 1924-3442 and TWA 3ABCD come close (Figure 6) with Hα emission strengths greater than -10Å, which are recorded in Table 5.

5.2. *Lithium (6708Å) age indicator*

Only ten objects had measurable lithium, with a typical measurement precision of 0.18Å. This is expected, given that the selection consists of stars close to the convective limit where lithium is fused very quickly (see Figure 7, where they are plotted against lithium-bearing stars from the Catalog of Nearby Suspected Young Stars from Riedel et al. submitted). With only three exceptions (a Tuc-Hor member and two stars that do not match any known groups), our ten lithium-detected stars are known or new members of the $\sim$12-Myr-old TW Hydra moving group, as outlined in Table 5. To define typical values for the groups, we computed a 15-element moving average and a 15-element moving standard deviation for each group, such that the value (and standard deviation) of each point on the curves are the average of the surrounding 15 points, and are given for the mean $V-K$ values of those 15 points. Interestingly, all of our detections lie below the curve for TW Hya members ($\sim$10 Myr) and above the curve for β Pic ($\sim$25 Myr). Our targets have among the lowest lithium EWs measured for TW Hydra and the highest lithium EW for a Tuc-Hor member which suggests our unidentified young stars are under 25 Myr old. This is not entirely unexpected, given the apparent spread in lithium measurements shown in Figure 7.

5.3. *Potassium (7699Å) gravity indicator*

The potassium 7699Å line[5] was measured for the entire sample, and results are shown in Figure 8. In order to determine a standard of youth, the potassium EW measurements are compared to measurements of objects in the Catalog of Suspected Nearby Young Stars in Riedel et al. (submitted), whose potassium measurements are largely from Riedel et al. (2014) and Shkolnik et al. (2009), plus the additional field star measurements used in Riedel et al. (2014). Both samples have relatively large uncertainties on the equivalent widths (0.2Å for Riedel et al. 2014, 0.24 or 0.16Å for Shkolnik et al. 2009, depending on the telescope) which, combined with intrinsic scatter, make the field star locus rather large (as defined by a 15-element moving average). Stars more than one standard deviation below the main sequence locus (as defined by a 15-element moving standard deviation) in Figure 8 are therefore treated as potentially low surface gravity objects and likely to be young, and this is used in the youth evaluation in Table 5. The lowest value, -0.07 ± 0.01Å, for SCR 2204-0711, is not shown in Figure 8 and suggests that the star is in fact a giant.

5.4. *Kinematic Results*

To supplement our radial velocities (Table 2, Section 4.1), ICRS positions and proper motions for these objects were obtained from the Fourth USNO Compiled Astrographic Catalog (UCAC4, Zacharias et al. 2013) and PPMXL (Roeser et al. 2010) catalogs. These are given in Table 1.

We use the LocAting Constituent mEmbers In Nearby Groups (LACEwING, Riedel et al. submitted) moving group identification code to evaluate membership probabilities in the NYMGs. LACEwING calculates up to four metrics of membership by comparing the proper motions, parallaxes, radial velocities, and space positions of targets (depending on what data is available) against predictions computed for a member of the group at that RA and DEC. These metrics are combined into a single goodness-of-fit value, and translated into a membership probability using the pre-calculated results of a simulation of 8 million stars.

Membership probabilities are calculated by taking the simulated stars and matching them to each of thirteen nearby young moving groups and three open clusters (Table 3), and then computing a membership probability based on the result of combining four goodness-of-fit scores. Therefore, for a group X, there is a histogram of all the simulated stars with their goodness-of-fit scores when matched to group X. The histogram records the percentage of stars in each bin that were actually members of group X, effectively making the LACEwING percentages contamination probabilities. LACEwING does not force all probabilities to add up to 100%, so there is still a chance that the stars will not match

[5] The other line in the doublet, potassium 7635Å, is within the atmospheric A band and not suitable for measurement.

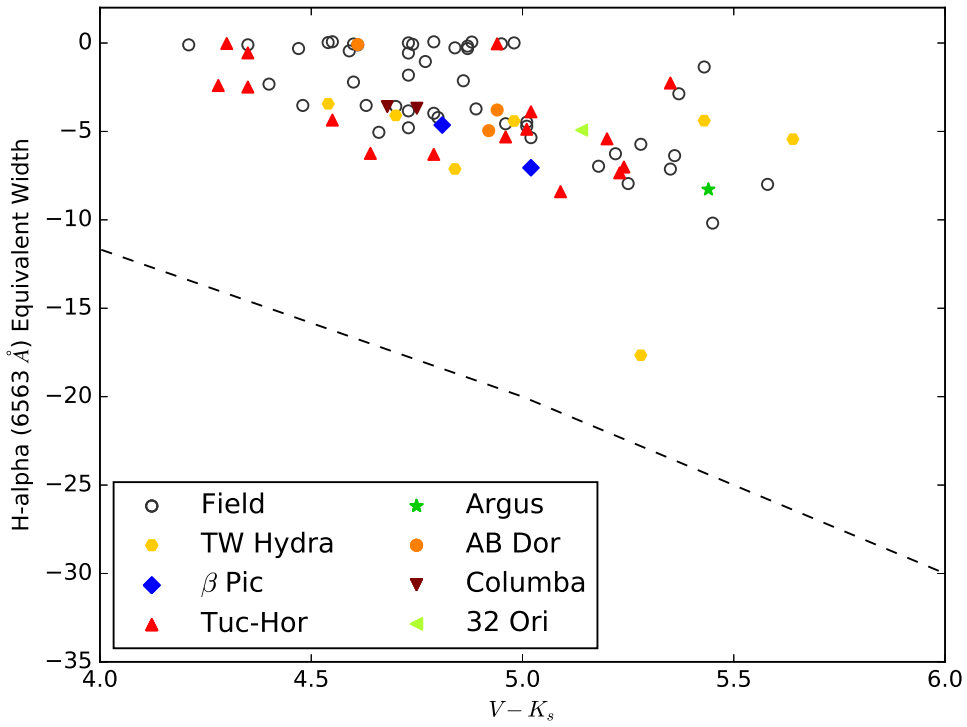

Figure 6. Hα equivalent widths versus $V-K$ color (as a proxy for spectral type), with veiling criterion (dashed line) from White & Basri (2003). All of these stars are post-T-Tauri stars, and the single star (represented by both measurements) that comes closest to the limit is TWA 3ABCD.

any known group, or add up to more than 100% if the uncertainties are larger than the simulation expected.

Table 3. Moving Groups and Open Clusters Considered by the LACEwING Code

Name	Age (Myr)	Ref
ϵ Chameleontis	5	Murphy et al. (2013)
η Chameleontis[a]	10	Murphy et al. (2013)
TW Hydra	10	Weinberger et al. (2013)
32 Orionis	20	Bell et al. (2015)
β Pictoris	25	Bell et al. (2015)
Octans	40	Murphy & Lawson (2015)
Tucana-Horologium	45	Bell et al. (2015)
Columba	45	Bell et al. (2015)
Carina	45	Bell et al. (2015)
Argus	50	Barrado y Navascués et al. (2004)
AB Doradus	150	Bell et al. (2015)
Carina-Near	200	Zuckerman et al. (2006)
Ursa Major	400	Jones et al. (2015)
Coma Berenices[a]	400	Kraus & Hillenbrand (2007)
χ^1 Fornax	525	Pöhnl & Paunzen (2010)
Hyades[a]	800	Brandt & Huang (2015)

Table 3 continued

Table 3 *(continued)*

Name	Age (Myr)	Ref

[a] Open Cluster

NOTE—Ages have been rounded to the nearest 5 Myr.

As shown in Riedel et al. (submitted), kinematic identification of young stars improves with more and higher-precision data. By including radial velocities, we significantly decrease the false positive rate. However, because LACEwING uses standard deviations in its four membership metrics, the lower quality of radial velocities (5 km s^{-1}) compared to the ones LACEwING is calibrated for (1 km s^{-1}) will result in better apparent matches and higher membership probabilities than would otherwise be expected.

LACEwING has two modes: one including a field star population 50 times the size of the NYMG population, implicitly assuming that the star under consideration might be a field interloper with coincidentally similar motions; and one for use if the star is already known to be young, where nearly all of the field star population is removed from consideration, leaving only a 1:1 contribution of field stars:NYMG members to represent the fact that Riedel et al. (submitted) found half of all young stars (there, defined as lithium-rich objects) were

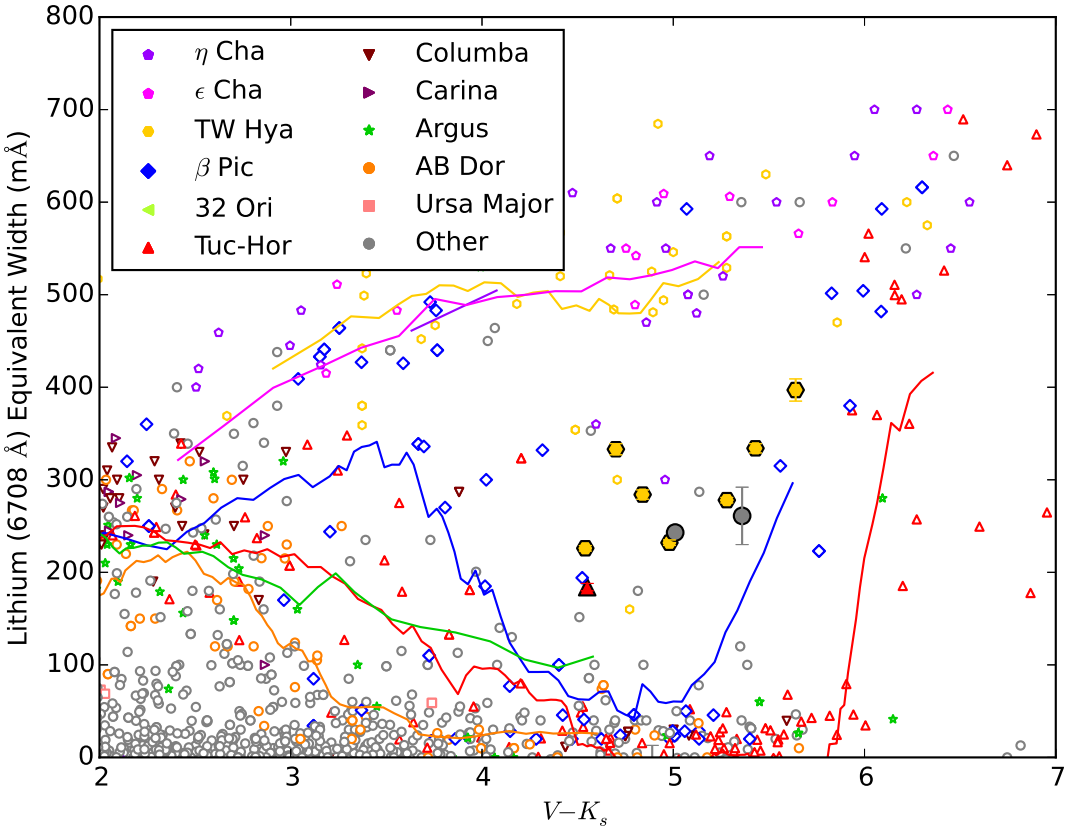

Figure 7. Lithium equivalent width versus $V - K$. Ten stars in our sample with measurable lithium are shown with shapes outlined in black. The smaller shapes are stars from the Catalog of Suspected Nearby Young Stars (Riedel et al. submitted), with 15-element moving averages plotted as rough trendlines for each group.

not members of any NYMG (see also Section 7), suggesting the presence of a young field. Stars with lithium detections or with potassium line strengths more than 1-σ weaker than field stars were assumed to be young. All other stars were run through LACEwING's field star mode.

For 13 stars with parallaxes (mostly from Riedel et al. 2014), we can also compute full UVW space velocities and space positions following the matrix method of Johnson & Soderblom (1987). These are given in Table 4.

Table 4. $UVWXYZ$ space velocities and positions

Name	U (km s^{-1})	V (km s^{-1})	W (km s^{-1})	X (pc)	Y (pc)	Z (pc)
SCR 0017-6645	-17.7±2.5	-8.8±3.0	2.9±4.3	15.6±1.1	-19.8±1.4	-30.1±2.1
GJ 2006A	-11.6±0.8	-14.9±1.0	24.1±4.6	4.1±0.2	-1.1±0.1	-32.1±1.8
GJ 2006B	-12.2±1.3	-13.4±1.2	-8.0±6.1	4.1±0.2	-1.1±0.1	-32.1±1.8
HIP 3556	-11.3±1.7	-18.7±2.7	4.8±4.5	9.8±1.1	-13.9±1.5	-37.2±4.1
BAR 161-12	-13.0±2.0	-9.8±1.1	-17.7±5.3	-10.1±0.1	5.2±0.0	-27.4±0.2
SCR 1012-3124AB	-14.7±1.4	-17.8±5.2	-7.8±2.3	-2.4±0.2	-51.0±4.9	18.8±1.8
SCR 1121-3845	-13.9±1.0	-16.6±2.0	-6.7±1.0	14.8±0.7	-58.2±2.6	22.8±1.0
TWA 5ABC	-11.9±0.7	-17.7±1.9	-5.9±1.0	11.6±0.4	-43.8±1.5	21.6±0.8
RX 1132-2651A	-14.7±1.6	-17.9±2.2	-8.1±1.9	8.2±0.4	-38.7±1.9	25.5±1.2
2MASS 1207-3247	-18.4±1.1	2.1±2.4	-17.5±1.5	17.9±0.5	-43.6±1.1	26.3±0.7
SCR 1425-4113AB	-0.9±2.9	-24.5±2.5	-4.6±1.4	49.8±3.2	-39.9±2.6	21.1±1.4
SCR 2010-2801AB	-2.6±3.6	-11.7±1.3	-12.0±2.2	41.0±2.7	10.3±0.7	-23.0±1.5
L 755-19	-28.9±4.4	-20.7±2.9	-1.1±2.7	14.0±0.4	9.2±0.3	-8.5±0.3

Table 4 continued

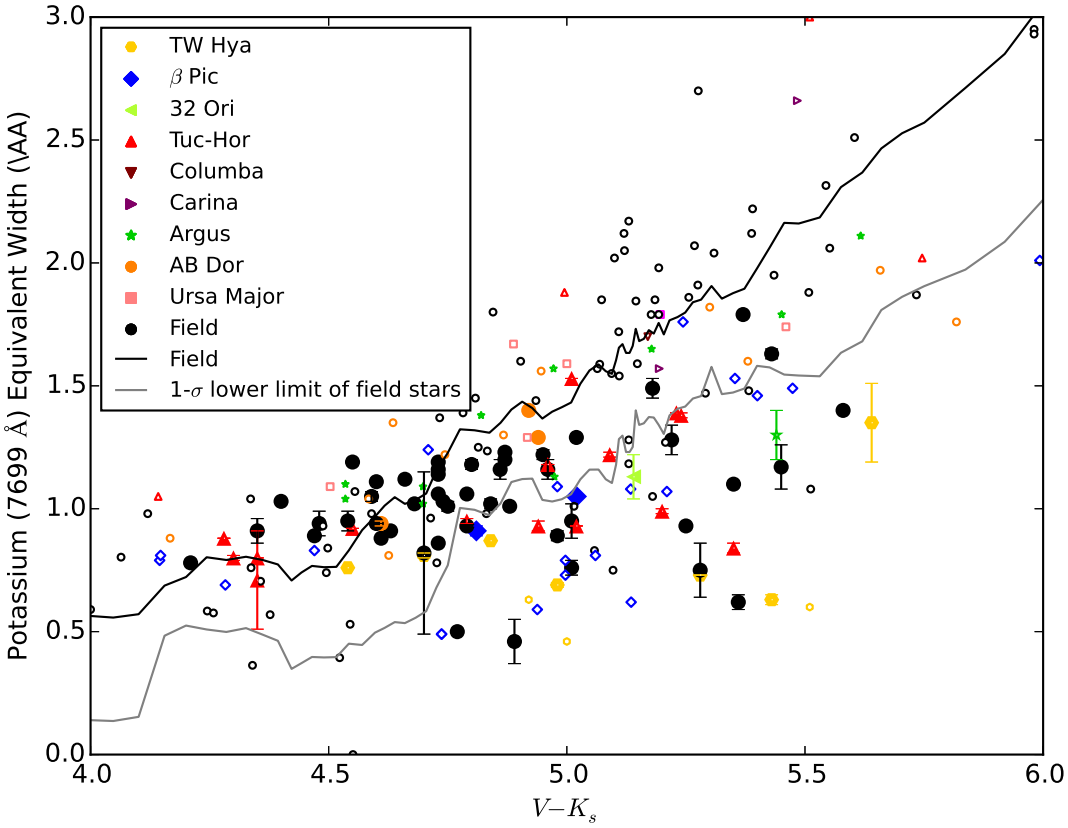

Figure 8. Potassium equivalent width versus $V-K$. Stars appear according to Figure 7. The black curve is a 15-element windowed average fit to the field stars from the Catalog of Nearby Young Stars (Riedel et al. submitted) and the sample field stars in Riedel et al. (2014). The main sequence locus has some width due to imprecise measurements in the CTIO 1.5m RCSpec data from Riedel et al. (2014), and intrinsic scatter amongst group members. The gray line represents the 15-element windowed standard deviation of field stars and is roughly 0.5Å. Stars that lie below the line (i.e. with weaker potassium absorption) are considered young.

Table 4 *(continued)*

Name	U (km s^{-1})	V (km s^{-1})	W (km s^{-1})	X (pc)	Y (pc)	Z (pc)

NOTE—All values computed using right-handed coordinates, where U/X is toward the center of the Galaxy, V/Y in the direction of motion, and W/Z toward the north Galactic pole. Memberships for stars are given in Table 5

6. DISCUSSION

Our spectroscopic indicators are only sensitive to the youngest stars in this sample of hot M dwarfs. As shown in Figure 7, we should only expect to detect significant lithium in members of the youngest groups: ϵ Cha (5 Myr), the η Cha open cluster (8 Myr), and TW Hya (10 Myr); our sample spans a range of temperatures where lithium is destroyed very quickly. None of our stars are young enough to meet the Hα EW veiling criterion (Figure 6); all are post-T-Tauri stars. The relatively low precision of our potassium line measurements (Figure 8) demonstrates that Tuc-Hor (45 Myr) is the oldest group for which significant numbers of stars fall below the field distribution. Any star that meets any of the spectroscopic criteria for youth is therefore definitely young, and most likely in Argus (50 Myr old) or the younger NYMGs (see Table 3). Members of older NYMGs like AB Doradus (150 Myr old) should not meet our spectroscopic young criterion. These objects may still be identified by kinematics, though it is important to reiterate that kinematic techniques make no comment on the actual age of stars.

We take the most likely group reported by the LACEwING kinematic code as the correct membership, unless it is below 20% probability, or the star is clearly younger than the most likely membership.

In total, we have identified 44 young systems (46 young stars) using the SALT spectroscopy, as shown in Table 5.

Table 5. Youth Properties

Name	Youth	Literature		LACEwING		Kine. dist	Kine. RV	Measured RV
	Flags	Membership	Ref.	Membership	Prob.	(pc)	(km s^{-1})	(km s^{-1})
SCR 0017-6645	K	β Pic	1	Tuc-Hor	50	48.2±4.5	+7.4±3.5	−4.8±5.6
GJ 2006A	K	β Pic	2	β Pic[a]	0	35.8±3.3	+8.3±1.7	−24.9±4.6
GJ 2006B	K	β Pic	2	β Pic	49	34.3±3.2	+8.3±1.6	+6.9±6.1
HIP 3556		Tuc-Hor	3	Tuc-Hor	74	40.8±3.8	+5.7±3.4	−0.7±4.9
SCR 0106-6346				Tuc-Hor	25	39.2±4.9	+8.7±3.5	+13.3±5.2
[PS78] 190								+3.6±5.4
BAR 161-12	K	β Pic	4					+19.0±5.8
GIC 138								−26.4±7.2
L 173-39								+33.6±5.5
SCR 0149-5411				Tuc-Hor	22	37.1±4.9	+9.4±3.3	+2.1±4.1
SCR 0152-5950		Tuc-Hor	5	Tuc-Hor	38	39.1±5.5	+10.1±3.3	+14.0±5.3
SCR 0212-5851		Tuc-Hor	6					+4.5±5.0
SCR 0213-4654								+9.4±6.0
SCR 0215-0929		Tuc-Hor	1					+15.4±5.5
SCR 0220-5823		Tuc-Hor	6	Tuc-Hor	27	43.4±6.8	+11.3±3.3	+18.3±6.3
SCR 0222-6022	K	Tuc-Hor	6	Tuc-Hor[a]	42	30.7±4.9	+11.5±3.3	+28.6±7.0
2MASS 0236-5203	L	Tuc-Hor	7	Tuc-Hor	95	41.8±6.3	+11.7±3.1	+12.9±5.5
LP 886-73	K							−16.5±6.4
SCR 0248-3404	K			Tuc-Hor	87	46.2±5.4	+11.0±2.7	+14.5±5.5
SCR 0254-5746								+0.1±5.0
2MASS 0254-5108A		Tuc-Hor	7	Tuc-Hor	37	44.0±6.9	+12.6±3.1	+13.0±5.1
SCR 0256-6343		Tuc-Hor	8					−10.9±6.0
LP 831-35				AB Dor	32	27.4±0.1	+23.0±1.9	+25.5±6.1
2MASS 0510-2340A		Columba	1	Columba	27	50.2±4.8	+23.4±1.9	+18.8±5.2
2MASS 0510-2340B		Columba	1	Columba	20	58.4±5.9	+23.4±1.9	+15.6±7.5
SCR 0522-0606	K			32 Ori	59	87.6±6.5	+21.1±0.4	−1.5±5.0
SCR 0711-3510AB		AB Dor	1					+4.1±5.0
SCR 0844-0637								−18.0±2.0
LP 728-71								−5.6±3.4
SCR 1012-3124AB	LK	TW Hya	2	TW Hya	90	41.8±8.6	+15.7±2.3	+14.6±5.5
TWA 3ABCD	LKh	TW Hya	9	TW Hya	57	34.5±6.4	+12.6±2.2	+14.5±2.5
SCR 1121-3845	L	TW Hya	10	TW Hya	100	56.0±10.2	+12.1±2.2	+9.5±2.2
TWA 5ABC	L	TW Hya	11	TW Hya	100	47.4±8.6	+11.1±2.2	+10.2±2.2
RX 1132-3019	L	TW Hya	12	TW Hya	78	43.6±7.9	+10.7±2.1	+15.8±4.7
RX 1132-2651A	LK	TW Hya	13	TW Hya	88	38.6±7.6	+10.3±2.1	+7.8±2.5
SIPS 1145-4055								+14.2±6.2
LP 851-410	K							−36.7±4.3
SCR 1200-1731	LK							+20.1±2.4
2MASS 1207-3247	K	TW Hya	14					−16.4±2.9
L 758-107	K							−12.0±4.9
SCR 1230-3300								+20.7±2.2
SCR 1233-3641								+6.7±4.4
SCR 1237-4021	LK			TW Hya	88	61.4±10.6	+7.6±2.3	+11.3±2.4
SCR 1238-2703		AB Dor	1					+0.5±3.3
SCR 1316-0858								+6.1±4.9
SCR 1321-1052	K							+26.5±5.6

Table 5 continued

Table 5 *(continued)*

Name	Youth Flags	Literature Membership	Ref.	LACEwING Membership	Prob.	Kine. dist (pc)	Kine. RV (km s^{-1})	Measured RV (km s^{-1})
SCR 1421-0916	K							−4.3±4.3
SCR 1421-0755	K							−5.2±7.2
SCR 1425-4113AB	LK	TW Hya	2					+12.4±3.7
SCR 1438-3941								+36.6±5.9
LP 914-6								+17.5±4.1
SCR 1521-2514								−0.8±2.9
SCR 1708-6936		Tuc-Hor	1					+11.3±3.4
SCR 1816-6305								+33.5±0.9
SCR 1842-5554A	K	β Pic	1					+9.8±4.9
NLTT 47004AB								+21.0±4.0
SCR 1856-6922								+21.1±4.0
WT 625								−15.6±4.3
SCR 1922-6310		Tuc-Hor	1					+5.7±2.1
RX 1924-3442	Kh	β Pic	1					−7.7±5.7
SCR 1926-5331	K			Tuc-Hor	42	57.2±7.5	−2.8±3.9	−7.6±6.0
SCR 1938-2416								+14.4±3.9
SCR 1951-4025								+20.6±5.9
SCR 2004-6725A								+10.4±3.5
2MASS 2004-3356	K	β Pic	15	Argus	44	30.6±0.7	−18.4±1.8	−16.1±3.8
SCR 2008-3519	K			Tuc-Hor	29	54.3±6.6	−9.8±4.0	−5.9±6.3
SCR 2010-2801AB	K	β Pic	1					+1.0±4.2
L 755-19		Argus	2					−31.2±5.8
SCR 2107-7056				Tuc-Hor	23	50.0±4.6	+4.6±3.8	+3.3±4.6
SCR 2107-1304		β Pic	1					−3.7±4.8
LEHPM 1-4147								+12.4±4.0
SCR 2204-0711	K							
SCR 2237-2622	K	Argus	1	Tuc-Hor	33	44.8±0.5	−8.2±3.5	+3.4±5.0
SIPS 2258-1104								+20.2±5.5
LEHPM 1-5404				AB Dor	32	21.5±0.2	+15.0±1.9	+12.3±6.7
SCR 2328-6802		Tuc-Hor	1	Tuc-Hor	32	49.6±2.5	+6.3±3.7	+3.5±5.1
LTT 9582		AB Dor	1	AB Dor	31	23.3±0.1	+12.1±1.9	+8.7±5.3
G 275-71	K			Tuc-Hor[a]	48	29.7±0.9	−5.1±3.1	−2.9±7.7
LEHPM 1-6053								+25.2±5.7

NOTE—Membership flags are based on spectroscopic analysis (see Section 5) and are given as follows: (K) potassium EW below standard deviation of field value, (L) detectable lithium absorption, (h) Hα emission stronger than −10Å. Values are given in Table 6. Measured radial velocities are reprinted from Table 2. Membership references are to the first paper that identified the object as a member, and are 1.) Malo et al. (2013), 2.) Riedel et al. (2014), 3.) Zuckerman et al. (2001), 4.) Shkolnik et al. (2012), 5.) Kiss et al. (2011), 6.) Rodriguez et al. (2013), 7.) Torres et al. (2000), 8.) Kraus et al. (2014), 9.) de la Reza et al. (1989) 10.) Sterzik et al. (1999), 11.) Gregorio-Hetem et al. (1992), 12.) Looper et al. (2010), 13.) Webb et al. (1999), 14.) Song et al. (2003), 15.) Gagné et al. (2015)

[a] Initial match was to a different moving group; see Section 6 for details.

6.1. *TW Hya members (10 Myr)*

A number of known TW Hya systems are in our sample, and we reproduce membership for all but 2MASS 1207-3247 (TWA 23), which is also our only member without a lithium detection.

We have identified one new member of TW Hya. SCR 1237-4012 (Figure 9) is confirmed by its lithium absorption, low surface gravity from potassium absorption, and kinematic match (88%) to TW Hya.

SCR 1237-4012 is only 1957 arcseconds from TWA

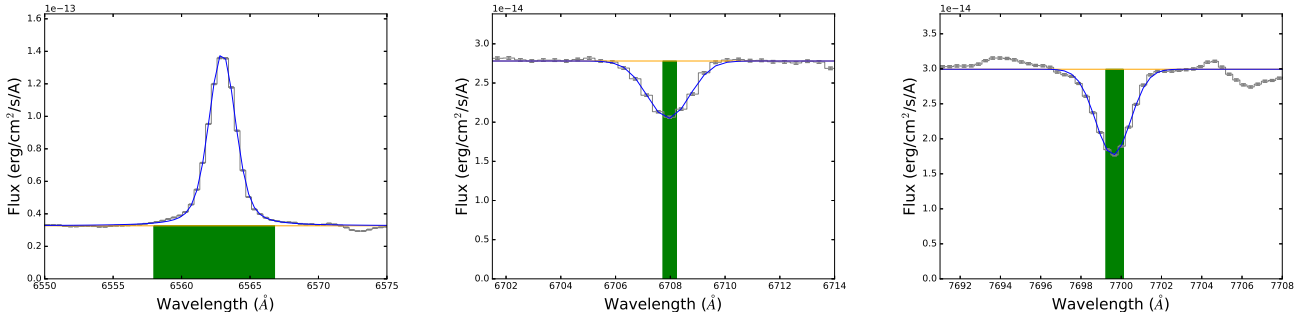

Figure 9. The measured Hα (6563 Å) EW, Li (6708Å) EW, and K I (7699Å) EW for SCR 1237-4021. The psuedocontinuum (yellow) and Voigt profile (blue) are fit to the observed spectrum (grey). The green rectangles approximate the EWs.

11ABC, a triple system comprised of an A0 star, and two M2.5 companions. As an A0 star, TWA 11A is the most massive member of TW Hya. At the measured distance of TWA 11A (71.6±1.4 pc, consistent with the kinematic estimate of 61±10 pc), the projected separation of SCR 1237-4012 is only 0.68 parsecs.

Following the discussion of Mamajek et al. (2013) and Jiang & Tremaine (2010), we estimate the mass of TWA 11A at 2.3 solar masses[6] and TWA 11B and C at 0.4 solar masses each based on fits to 10 Myr Baraffe & Chabrier (2010) isochrones. With a total system mass of 3 solar masses, the tidal radius should be 2 pc, and it is plausible that SCR 1237-4012 is an outer quadruple companion of the system. We note that given a population of 38 systems, within a 1σ volume of 3000 cubic parsecs (Riedel et al. submitted), the average separation between members of TW Hya should be on the order of 2.6 parsecs.

If we take the proper motion of TWA 11A (pmRA,pmDEC = -56.7 ± 0.3, -25.0 ± 0.2 mas yr^{-1} from van Leeuwen 2007) and SCR 1237-4012 (pmRA,pmDEC = -63.7 ± 1.1,-29.1 ± 1.1 mas yr^{-1} from Zacharias et al. 2013), the proper motions differ by 8 mas yr^{-1} (4σ), or 2.75 km s^{-1} transverse velocity if they are at the same distance. There are two RVs for TWA 11: 7.1 ± 1.1 km s^{-1} from Gontcharov (2006), and 9.4 ± 2.3 km s^{-1} from Kharchenko et al. (2007). If we compare the RVs to our RV for SCR 1237-4012, 11.3 ± 2.4 km s^{-1}, the two systems' space velocities (if at the same distance) are separated by either 5.0 km s^{-1} or 3.3 km s^{-1}. It is therefore somewhat less likely that the stars are in the same system, and more likely that they are either a chance alignment or that SCR 1237-4012 was ejected from the system within the past half million years.

A parallax measurement (and proper motion on a uniform system) of SCR 1237-4012 will do a great deal to determine if the 3D separation and space motion of SCR 1237-4012 is reasonable to make it a genuine companion to TWA 11A.

6.2. *32 Ori member (20 Myr)*

The 32 Orionis moving group is relatively unstudied, and currently has only 17 known or suspected members. We have found another potential member, SCR 0522-0606, a low-surface-gravity M dwarf based on its potassium EW. The radial velocity is a 4σ mismatch with LACEwING's expectations for a member of 32 Ori, but the quality of the proper motion agreement and resulting estimated spatial position still gives the star a 59% probability of membership.

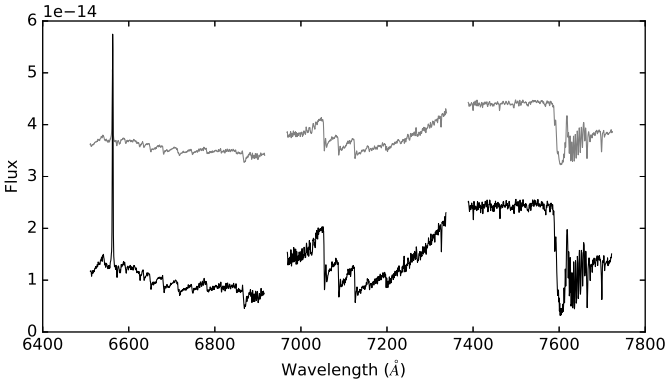

Figure 10. Spectra of GJ 2006A (top, gray) and GJ 2006B (bottom, black).

With its M2.5Ve spectral type, only three known members of the group have lower masses than SCR 0522-0606: two M3V stars, 2MASS J05253253+0625336 and 2MASS J05194398+0535021 (Bell et al. 2015), and one L1 low gravity brown dwarf (Burgasser et al. 2016). This is thus a useful benchmark object for the lower-mass end of the system.

6.3. *β Pic member (25 Myr)*

The GJ 2006 system is a common proper motion visual binary that Riedel et al. (2014) identified as β Pic members. For unknown reasons, our radial velocity for the A component is discrepant with both the B component and membership in β Pic, regardless of the spectral region fit or combination of comparison stars. It is not clear why this velocity is different, as both components appear to be M dwarfs with Hα in emission represented here by high-SNR spectra (Figure 10); further study is needed. For our purposes, we presume this velocity is in error, and identify both objects as β Pic members in Table 5.

6.4. *Tuc-Hor members (45 Myr)*

2MASS 0236-5203 was one of the first identified members of Tuc-Hor (Zuckerman et al. 2001), and we reproduce

[6] based on http://www.pas.rochester.edu/~emamajek/spt/A0V.txt, checked 20 Sep 2016

that membership here. That it has a measurable lithium absorption feature is surprising given the age of Tuc-Hor, although not without precendent, as can be seen in Figure 7, and by existing lithium measurements of 2MASS 0236-5203 from Torres et al. (2006) and Mentuch et al. (2008). It has a 23% probability of membership in the younger β Pic moving group, but we see no concrete reason to prefer that over Tuc-Hor membership.

SCR 0222-6022 has been considered as a member of Tuc-Hor before, by Rodriguez et al. (2013), Kraus et al. (2014), and Malo et al. (2014). The first two papers rejected that membership. With our new radial velocity, we find a 93% chance of membership in AB Dor, and only 42% in Tuc-Hor. However, SCR 0222-6022 has low surface gravity according to the potassium feature, which indicates it is more likely a younger star and a member of the younger Tuc-Hor NYMG.

In addition to recovering seven known members, we identify nine new members of Tuc-Hor:

SCR 0017-6645 (50%) was previously identified as a member of β Pic by Malo et al. (2013) and Riedel et al. (2014). We find only a 19% probability that it is a member of β Pic using our new radial velocity (-4.8 ± 5.6 km s^{-1}). If we take a weighted mean of our radial velocity with the radial velocity from Malo et al. (2013) (11.4 ± 0.8 km s^{-1}), the star is still more likely to be a member of Tuc-Hor. Given that this was one of the stars we removed from our fitting process in Section 4.1, it may be that our radial velocity is in error. However, if we use only Malo's radial velocity, the star has only a marginally higher probability (73%) of membership in β Pic than Tuc-Hor (68%).

Similarly, G 275-71 matches best to AB Dor (73%), but given its low surface gravity, it is more likely to be a member of Tuc-Hor (48%).

SCR 2237-2622 was previously identified by Malo et al. (2013) as a member of the Argus moving group. LACEwING results indicate a probability of 33% in Tuc-Hor, 32% in AB Dor, and no probability of membership in Argus.

SCR 0106-6346, SCR 0149-5411, SCR 0248-3404, SCR 1926-5331, SCR 2008-3519, and SCR 2107-7056 have never previously been identified as young stars. We note that SCR 0248-3404 was rejected as a member of Tuc-Hor by Kraus et al. (2014), and identified as an ambiguous nonmember by Malo et al. 2013; their published radial velocities $+23.3\pm0.5$ and $+14.6\pm0.3$ km s^{-1} (respectively) differ by nearly 11σ. Malo et al. (2014) found the system to be a single-lined spectroscopic binary (SB1). Our result ($+14.5\pm5.5$ km s^{-1}) is closer to that of Malo et al. (2013).

6.5. *Columba members (45 Myr)*

We find one member of the Columba moving group: 2MASS 0510-2340AB. It was identified as such by Malo et al. (2013) and we reproduce that membership for both components. Despite being the fainter star of the pair, the B component has an earlier spectral type both here and in Malo et al. (2013). This would suggest that they are actually two separate star systems, but their proper motions, kinematic distances, and radial velocities are identical at the 1-σ level, and they are separated by only 27 arcsec. More study of this system is needed.

6.6. *Argus members (50 Myr)*

2MASS 2004-3356 was identified as an X-ray active (and therefore probably young) star by Riaz et al. (2006) and Haakonsen & Rutledge (2009), and as a member of β Pic by Gagné et al. (2015). Our radial velocity (-16 km s^{-1}) is inconsistent with membership in β Pic, where -6 km s^{-1} would be expected, and it has only a 14% probability of membership in β Pic according to LACEwING. With its low surface gravity and 44% probability of membership in Argus, it is the only new member of Argus we have identified in this survey.

6.7. *AB Dor members (150 Myr)*

Two of the members of AB Dor identified here are new. LP 831-35 and LEHPM 1-5404 are not known as low gravity objects, which is consistent with their age.

6.8. *Young Nonmembers*

Perhaps most surprisingly, 14 of our stars are young – under 50 Myr old as inferred from their potassium measurements – but are not members of any NYMG according to their kinematics.

Two of these stars have lithium detections and must therefore be very young; most likely younger than Tuc-Hor (45 Myr): SCR 1425-4113AB and SCR 1200-1731. SCR 1425-4113AB was identified by Riedel et al. (2014) as a young star with potential kinematic matches to β Pic and TW Hya. Based on its overluminosity on a color-magnitude diagram that placed it brighter than the TW Hya isochrone, it was determined more likely to be a TW Hya member despite its distance from the rest of the TW Hya members. Malo et al. (2014) disputed this, placing the system in β Pic. With our new radial velocity, we find no probability of membership in either group, although the star remains under 25 Myr old according to its spectra. SCR 1200-1731, despite a spatial location and lithium measurement (Figure 11) that would likely make it a TW Hya member, has a radial velocity ($+20.1$ km s^{-1}) that disqualifies it entirely from membership in that group.

As mentioned in Section 6.1, we did not reproduce the membership of 2MASS 1207-3247 in TW Hya. Our radial velocity for 2MASS 1207-3247 (-16.4 ± 2.9) is very discrepant with the previously reported radial velocity $+8.5\pm1.2$ (Malo et al. 2013). If we combine that measurement with ours into a weighted mean ($+4.8\pm8.8$), we find a 100% probability of membership in TW Hya. If we remove that radial velocity, we find that the proper motions on their own are also discrepant with membership in TW Hya. It is worth noting that this was one of the stars we removed from our RV comparisons in 4.1.

BAR 161-12, SCR 1842-5554A, RX 1924-3442, and SCR 2010-2801AB have previously been identified as β Pic members, but are not members based on our new radial velocities. All of them (except BAR 161-12, which matches nothing) still match β Pic, though with probabilities too low to be meaningful.

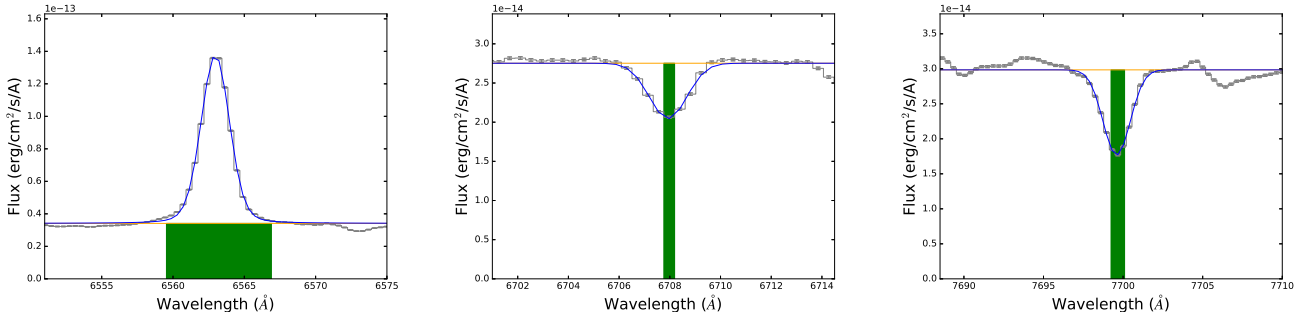

Figure 11. The measured Hα (6563 Å) EW (top), Li (6708Å) EW, and K I (7699Å) EW for SCR 1200-1731. The psuedocontinuum (yellow) and Voigt profile (blue) are fit to the observed spectrum (grey). The green rectangles approximate the EWs.

L 755-19 was identified by Riedel et al. (2014) as a potential member of Argus, but with RV has a membership probability of only 19%.

LP 886-73, LP 851-410, L 758-107, SCR 1321-1052, SCR 1421-0755, and SCR 1421-0916 have never been suspected of membership in any moving group before, and their only claim to youth is the fact that they have low surface gravity according to our potassium measurements. While these identifications might possibly be spurious, we believe that we have demonstrated this search methodology's ability to identify and recover genuinely young stars, and that these stars are therefore also young field stars.

6.9. *Giants*

The negative potassium EW (Table 6) measured for SCR 2204-0711 (as well as our Hα EW, and large and uncertain radial velocity in Table 2) is actually the result of the measurement code seeking out a completely different feature. This object appears to have NO measurable potassium absorption, and is likely to be a giant or supergiant, not a young star. This object has a spectral type of K9 but the colors of an M1-M6 dwarf.

7. CONCLUSIONS

We have obtained low-resolution red optical spectroscopy of 79 potentially nearby M dwarfs in 77 star systems. With that spectroscopy, we measured an age indicator, Li 6708Å; a gravity indicator, K I 7699Å; an activity indicator, Hα 6563Å; and 5 km s^{-1} precision radial velocities for every star in our sample.

Using that information, we have identified 44 young star systems: seven members of TW Hydra, one member of β Pic, one member of 32 Ori, 16 members of Tuc-Hor, one member of Columba, one member of Argus, three members of AB Dor, 14 young systems that we cannot place among the nearby young moving groups; by adding radial velocities and spectroscopic confirmation, we reinforce the strength of the membership identifications. Of the young systems, 12 are new moving group members, including one new member of TW Hya, one new member of 32 Ori, nine new members of Tuc-Hor, one new member of Argus, and two new members of AB Dor. We have also discovered one giant. This study proves that the selection cuts imposed by the TINYMO survey are extremely effective at identifying young stars, considering the ratio of field stars to young stars is 25:1 (Riedel et al. submitted) in the Solar Neighborhood.

We find that the new TW Hya member, SCR 1237-4012, is potentially within the tidal radius of the triple-star system TWA 11, and may be a fourth member or recently ejected object. We have also identified nine new members of Tuc-Hor, making the numerically largest known moving group (209 systems, Riedel et al. submitted; now 218) even larger. And we have added the third-lowest-mass member of the poorly explored 32 Ori moving group.

We also find further confirmation that a large number of young systems are not identifiably members of any known NYMGs – 32% (30% if we allow for 2MASS 1207-3247 as an actual member of TW Hya) of our young star systems are not members of any NYMG. This has been noticed before. Riedel et al. (submitted) used a catalog constructed from NYMG membership papers, selected a sample of spectroscopically young (defined as having detectable lithium) and high confidence "bona-fide" members, and found that more than half of the systems were *not* members of any known NYMGs when analyzed uniformly with any publicly available moving group identification code. Our sample here is unlike the samples provided by most moving group identification papers. We did not start by kinematically identifying stars in a proper motion sample and then following up only likely candidates with spectroscopy; rather, our sample is biased only to bright low-proper-motion objects. Given that these stars genuinely appear to be young, further work is necessary to determine the true nature of these stars.

8. ACKNOWLEDGEMENTS

All of the observations reported in this paper were obtained with the Southern African Large Telescope (SALT), which is a partnership between the South African Astronomical Observatory and 11 international partners, under program codes 2014-1-AMNH-002 and 2014-2-AMNH-002. The generosity of the late Paul Newman and the Newman Foundation has made AMNH's participation in SALT possible. PyRAF is a product of the Space Telescope Science Institute, which is operated by AURA for NASA. ARR would like to thank Noel Richardson for help with flux calibration and RV calibration of the data, Jamie McDonald for editorial assistance, and Michael Shara for help with the data acquisition.

Software: astropy (Astropy Collaboration et al. 2013), LACEwING (Riedel et al. submitted), MATCHSTAR (Riedel et al. 2014), PHEW (Alam & Douglas 2016), PyRAF, PySpecKit (Ginsburg & Mirocha 2011)

Facility: SALT (RSS)

REFERENCES

Alam, M., & Douglas, S. 2016, PHEW: PytHon Equivalent Widths, Zenodo, doi:10.5281/zenodo.47889. http://dx.doi.org/10.5281/zenodo.47889

Alksnis, A., Balklavs, A., Dzervitis, U., et al. 2001, Baltic Astronomy, 10, 1

Astropy Collaboration, Robitaille, T. P., Tollerud, E. J., et al. 2013, A&A, 558, A33

Baraffe, I., & Chabrier, G. 2010, A&A, 521, A44

Barrado y Navascués, D., Stauffer, J. R., & Jayawardhana, R. 2004, ApJ, 614, 386

Bell, C. P. M., Mamajek, E. E., & Naylor, T. 2015, MNRAS, 454, 593

Brandt, T. D., & Huang, C. X. 2015, ApJ, 807, 24

Buckley, D. A. H., Swart, G. P., & Meiring, J. G. 2006, in Society of Photo-Optical Instrumentation Engineers (SPIE) Conference Series, Vol. 6267, Society of Photo-Optical Instrumentation Engineers (SPIE) Conference Series, 0

Burgasser, A. J., Lopez, M. A., Mamajek, E. E., et al. 2016, ApJ, 820, 32

Cutri, R. M., Skrutskie, M. F., van Dyk, S., et al. 2003, 2MASS All Sky Catalog of point sources. (NASA/IPAC Infrared Science Archive. http://irsa.ipac.caltech.edu/applications/Gator/)

de la Reza, R., Torres, C. A. O., Quast, G., Castilho, B. V., & Vieira, G. L. 1989, ApJL, 343, L61

Faherty, J. K., Riedel, A. R., Cruz, K. L., et al. 2016, ApJS, 225, 10

Gagné, J., Lafrenière, D., Doyon, R., Malo, L., & Artigau, É. 2014, ApJ, 783, 121

—. 2015, ApJ, 798, 73

Ginsburg, A., & Mirocha, J. 2011, PySpecKit: Python Spectroscopic Toolkit, Astrophysics Source Code Library, , , ascl:1109.001

Gontcharov, G. A. 2006, Astronomy Letters, 32, 759

Gregorio-Hetem, J., Lepine, J. R. D., Quast, G. R., Torres, C. A. O., & de La Reza, R. 1992, AJ, 103, 549

Haakonsen, C. B., & Rutledge, R. E. 2009, ApJS, 184, 138

Hambly, N. C., Henry, T. J., Subasavage, J. P., Brown, M. A., & Jao, W. 2004, AJ, 128, 437

Hambly, N. C., Irwin, M. J., & MacGillivray, H. T. 2001a, MNRAS, 326, 1295

Hambly, N. C., MacGillivray, H. T., Read, M. A., et al. 2001b, MNRAS, 326, 1279

Henden, A. A., Templeton, M., Terrell, D., et al. 2016, VizieR Online Data Catalog, 2336

Henry, T. J., Kirkpatrick, J. D., & Simons, D. A. 1994, AJ, 108, 1437

Henry, T. J., Walkowicz, L. M., Barto, T. C., & Golimowski, D. A. 2002, AJ, 123, 2002

Hinkle, K. H., Wallace, L., & Livingston, W. 2003, in Bulletin of the American Astronomical Society, Vol. 35, American Astronomical Society Meeting Abstracts, 1260

Jiang, Y.-F., & Tremaine, S. 2010, MNRAS, 401, 977

Johnson, D. R. H., & Soderblom, D. R. 1987, AJ, 93, 864

Jones, J., White, R. J., Boyajian, T., et al. 2015, ArXiv e-prints, arXiv:1508.05643

Kharchenko, N. V., Scholz, R.-D., Piskunov, A. E., Röser, S., & Schilbach, E. 2007, Astronomische Nachrichten, 328, 889

Kirkpatrick, J. D., Henry, T. J., & McCarthy, Jr., D. W. 1991, ApJS, 77, 417

Kiss, L. L., Moór, A., Szalai, T., et al. 2011, MNRAS, 411, 117

Kobulnicky, H. A., Nordsieck, K. H., Burgh, E. B., et al. 2003, in Society of Photo-Optical Instrumentation Engineers (SPIE) Conference Series, Vol. 4841, Instrument Design and Performance for Optical/Infrared Ground-based Telescopes, ed. M. Iye & A. F. M. Moorwood, 1634–1644

Kraus, A. L., & Hillenbrand, L. A. 2007, AJ, 134, 2340

Kraus, A. L., Ireland, M. J., Cieza, L. A., et al. 2014, ApJ, 781, 20

Looper, D. L., Mohanty, S., Bochanski, J. J., et al. 2010, ApJ, 714, 45

Malo, L., Artigau, É., Doyon, R., et al. 2014, ApJ, 788, 81

Malo, L., Doyon, R., Lafrenière, D., et al. 2013, ApJ, 762, 88

Mamajek, E. E., Bartlett, J. L., Seifahrt, A., et al. 2013, AJ, 146, 154

Mentuch, E., Brandeker, A., van Kerkwijk, M. H., Jayawardhana, R., & Hauschildt, P. H. 2008, ApJ, 689, 1127

Murphy, S. J., & Lawson, W. A. 2015, MNRAS, 447, 1267

Murphy, S. J., Lawson, W. A., & Bessell, M. S. 2010, MNRAS, 406, L50

—. 2013, MNRAS, 435, 1325

Nidever, D. L., Marcy, G. W., Butler, R. P., Fischer, D. A., & Vogt, S. S. 2002, ApJS, 141, 503

Pöhnl, H., & Paunzen, E. 2010, A&A, 514, A81

Riaz, B., Gizis, J. E., & Harvin, J. 2006, AJ, 132, 866

Riedel, A. R. 2012, PhD thesis, Georgia State University

Riedel, A. R., Blunt, S. C., Rice, E. L., Cruz, K. L., & Faherty, J. K. submitted, AJ

Riedel, A. R., Murphy, S. J., Henry, T. J., et al. 2011, AJ, 142, 104

Riedel, A. R., Finch, C. T., Henry, T. J., et al. 2014, AJ, 147, 85

Rodriguez, D. R., Bessell, M. S., Zuckerman, B., & Kastner, J. H. 2011, ApJ, 727, 62

Rodriguez, D. R., Zuckerman, B., Kastner, J. H., et al. 2013, ApJ, 774, 101

Roeser, S., Demleitner, M., & Schilbach, E. 2010, AJ, 139, 2440

Samus, N. N., Durlevich, O. V., & et al. 2012, VizieR Online Data Catalog, 1, 2025

Schlieder, J. E., Lépine, S., Rice, E., et al. 2012, AJ, 143, 114

Schlieder, J. E., Lépine, S., & Simon, M. 2010, AJ, 140, 119

Schneider, A., Song, I., Melis, C., Zuckerman, B., & Bessell, M. 2012, ApJ, 757, 163

Shkolnik, E., Liu, M. C., & Reid, I. N. 2009, ApJ, 699, 649

Shkolnik, E. L., Anglada-Escudé, G., Liu, M. C., et al. 2012, ApJ, 758, 56

Song, I., Zuckerman, B., & Bessell, M. S. 2003, ApJ, 599, 342

Sterzik, M. F., Alcalá, J. M., Covino, E., & Petr, M. G. 1999, A&A, 346, L41

Torres, C. A. O., da Silva, L., Quast, G. R., de la Reza, R., & Jilinski, E. 2000, AJ, 120, 1410

Torres, C. A. O., Quast, G. R., da Silva, L., et al. 2006, A&A, 460, 695

van Leeuwen, F. 2007, A&A, 474, 653

Webb, R. A., Zuckerman, B., Platais, I., et al. 1999, ApJL, 512, L63

Weinberger, A. J., Anglada-Escudé, G., & Boss, A. P. 2013, ApJ, 762, 118

West, A. A., Hawley, S. L., Bochanski, J. J., et al. 2008, AJ, 135, 785

White, R. J., & Basri, G. 2003, ApJ, 582, 1109

Zacharias, N., Finch, C. T., Girard, T. M., et al. 2013, AJ, 145, 44

Zacharias, N., Monet, D. G., Levine, S. E., et al. 2005, VizieR Online Data Catalog, 1297

Zuckerman, B., Bessell, M. S., Song, I., & Kim, S. 2006, ApJL, 649, L115

Zuckerman, B., Song, I., & Webb, R. A. 2001, ApJ, 559, 388

Table 6. SALT Equivalent Widths

Designated	Obs	H-α EW (Å)		Li EW (mÅ)		K I EW (Å)	
Name	Date	Measured	Weighted	Measured	Weighted	Measured	Weighted
SCR 0017-6645	2013-08-21	-6.30	-6.30±0.01	…	…	0.96	0.95±0.01
SCR 0017-6645	2013-08-21	-6.30		…		0.94	
GJ 2006A	2013-08-18	-4.63	-4.64±0.01	…	…	0.93	0.91±0.02
GJ 2006A	2013-08-18	-4.65		…		0.88	
GJ 2006B	2013-08-22	-7.05	-7.05±0.01	…	…	1.06	1.05±0.01
GJ 2006B	2013-08-22	-7.06		…		1.05	
HIP 3556	2013-08-22	-0.57	-0.56±0.01	…	…	0.80	0.80±0.01
HIP 3556	2013-08-22	-0.54		…		0.79	
SCR 0106-6346	2013-08-18	-4.90	-4.88±0.02	…	…	1.53	1.53±0.01
SCR 0106-6346	2013-08-18	-4.86		…		1.53	
[PS78] 190	2013-08-22	-0.57	-0.57±0.01	…	…	1.18	1.19±0.01
[PS78] 190	2013-08-22	-0.56		…		1.20	
BAR 161-12	2013-08-21	-7.56	-7.40±0.29	…	…	1.10	1.10±0.01
BAR 161-12	2013-08-21	-6.89		…		1.10	
GIC 138	2014-01-17	+0.06	+0.08±0.01	…	…	1.20	1.17±0.01
GIC 138	2014-01-17	+0.08		…		1.17	
L 173-39	2013-08-22	-2.33	-2.33±0.01	…	…	1.03	1.03±0.01
L 173-39	2013-08-22	-2.32		…		1.02	
SCR 0149-5411	2014-01-18	-0.03	-0.03±0.01	…	…	0.80	0.81±0.01
SCR 0149-5411	2014-01-18	-0.03		…		0.81	
SCR 0152-5950	2013-08-22	-2.62	-2.49±0.13	…	…	0.51	0.71±0.20
SCR 0152-5950	2013-08-22	-2.36		…		0.91	
SCR 0212-5851	2013-08-20	-3.60	-3.54±0.06	…	…	0.88	0.92±0.05
SCR 0212-5851	2013-08-21	-3.47		…		0.98	
SCR 0213-4654	2013-12-01	-7.23	-6.86±0.29	…	…	1.45	1.49±0.04
SCR 0213-4654	2013-12-01	-6.64		…		1.53	
SCR 0215-0929	2013-08-23	-5.06	-5.05±0.01	…	…	1.11	1.12±0.01
SCR 0215-0929	2013-08-23	-5.04		…		1.13	
SCR 0220-5823	2013-08-22	-8.40	-8.41±0.01	…	…	1.23	1.22±0.01
SCR 0220-5823	2013-08-22	-8.41		…		1.21	
SCR 0222-6022	2013-08-23	-7.33	-7.34±0.01	…	…	1.39	1.39±0.01
SCR 0222-6022	2013-08-23	-7.35		…		1.39	
2MASS 0236-5203	2013-08-22	-4.36	-4.36±0.01	180	184±4	0.92	0.92±0.01
2MASS 0236-5203	2013-08-22	-4.36		188		0.91	
LP 886-73	2014-02-02	-7.97	-8.00±0.02	…	…	1.40	1.40±0.01
LP 886-73	2014-02-02	-8.02		…		1.41	
SCR 0248-3404	2013-08-21	-7.36	-6.93±0.37	…	…	1.38	1.38±0.01
SCR 0248-3404	2013-08-21	-6.61		…		1.39	
SCR 0254-5746	2013-08-21	+0.04	+0.02±0.02	…	…	0.92	0.96±0.04
SCR 0254-5746	2013-08-21	+0.01		…		0.99	
2MASS 0254-5108A	2013-08-22	-2.47	-2.40±0.06	…	…	0.88	0.88±0.01
2MASS 0254-5108A	2013-08-23	-2.34		…		0.89	
SCR 0256-6343	2013-08-21	-6.29	-6.26±0.03	…	…	1.22	1.28±0.06
SCR 0256-6343	2013-08-21	-6.24		…		1.33	
LP 831-35	2013-08-23	-4.88	-4.95±0.07	…	…	1.40	1.40±0.01
LP 831-35	2013-08-23	-5.02		…		1.40	
2MASS 0510-2340A	2013-08-23	-3.59	-3.59±0.01	…	…	1.02	1.02±0.01
2MASS 0510-2340A	2013-08-23	-3.59		…		1.03	
2MASS 0510-2340B	2014-02-27	-3.54		…		1.01	
2MASS 0510-2340B	2013-10-23	-3.84	-3.73±0.10	…	…	1.05	1.01±0.03

Table 6 continued

Table 6 *(continued)*

Designated	Obs	H-α EW (Å)		Li EW (mÅ)		K I EW (Å)	
Name	Date	Measured	Weighted	Measured	Weighted	Measured	Weighted
2MASS 0510-2340B	2013-10-23	-3.76		…		0.98	
2MASS 0510-2340B	2014-02-27	-3.67		…		1.01	
SCR 0522-0606	2013-12-02	-4.06	-5.32±0.97	…	…	1.05	1.15±0.09
SCR 0522-0606	2013-12-02	-6.06		…		1.23	
SCR 0711-3510AB	2014-04-11	-2.11	-2.13±0.02	…	…	1.20	1.16±0.04
SCR 0711-3510AB	2014-04-11	-2.16		…		1.13	
SCR 0844-0637	2014-02-18	-0.32	-0.31±0.01	…	…	1.20	1.20±0.01
SCR 0844-0637	2014-02-18	-0.30		…		1.19	
LP 728-71	2014-03-08	-0.04	-0.05±0.01	…	…	1.23	1.21±0.02
LP 728-71	2014-03-08	-0.06		…		1.20	
SCR 1012-3124AB	2014-03-15	-4.37	-4.39±0.02	329	334±5	0.61	0.63±0.02
SCR 1012-3124AB	2014-03-15	-4.41		339		0.64	
TWA 3ABCD	2014-02-17	-17.74	-17.66±0.08	281	278±3	0.73	0.73±0.01
TWA 3ABCD	2014-02-17	-17.58		275		0.73	
SCR 1121-3845	2014-02-15	-3.46	-3.44±0.02	229	226±3	0.76	0.76±0.01
SCR 1121-3845	2014-02-15	-3.42		223		0.77	
TWA 5ABC	2014-02-27	-4.20	-4.13±0.09	340	335±6	0.79	0.80±0.01
TWA 5ABC	2014-02-27	-4.01		327		0.82	
RX 1132-3019	2014-01-30	-5.50	-5.43±0.07	409	396±12	1.51	1.34±0.16
RX 1132-3019	2014-01-30	-5.37		384		1.18	
RX 1132-2651A	2014-02-27	-7.09	-7.12±0.03	278	283±5	0.87	0.87±0.01
RX 1132-2651A	2014-02-27	-7.16		289		0.87	
SIPS 1145-4055	2013-05-25	-1.48	-1.42±0.09	…	…	1.60	1.61±0.02
SIPS 1145-4055	2013-05-25	-1.27		…		1.65	
LP 851-410	2014-02-02	-2.03	-0.86±1.04	…	…	0.49	0.50±0.01
LP 851-410	2014-02-02	+0.06		…		0.50	
SCR 1200-1731	2014-01-30	-6.47	-6.34±0.11	231	266±31	0.64	0.60±0.03
SCR 1200-1731	2014-01-30	-6.25		294		0.58	
2MASS 1207-3247	2014-02-27	-2.83	-2.81±0.05	93	64±37	0.62	0.62±0.03
2MASS 1207-3247	2014-02-27	-2.79		22		0.66	
2MASS 1207-3247	2014-02-27	-3.95		-91		0.41	
2MASS 1207-3247	2014-02-27	-2.82		96		0.60	
L 758-107	2014-01-19	+0.06	+0.06±0.01	…	…	1.02	1.01±0.01
L 758-107	2014-01-19	+0.05		…		1.01	
SCR 1230-3300	2014-01-26	-0.33	-0.31±0.01	…	…	0.88	0.89±0.01
SCR 1230-3300	2014-01-26	-0.30		…		0.89	
SCR 1233-3641	2014-02-02	-3.62	-3.59±0.03	…	…	0.50	0.83±0.33
SCR 1233-3641	2014-02-02	-3.56		…		1.15	
SCR 1237-4021	2014-01-21	-4.39	-4.41±0.02	234	232±3	0.69	0.69±0.01
SCR 1237-4021	2014-01-21	-4.43		229		0.70	
SCR 1238-2703	2014-01-14	-2.20	-2.21±0.01	…	…	1.12	1.11±0.01
SCR 1238-2703	2014-01-14	-2.22		…		1.10	
SCR 1316-0858	2014-03-16	-2.84	-2.87±0.03	…	…	1.78	1.79±0.01
SCR 1316-0858	2014-03-16	-2.90		…		1.80	
SCR 1321-1052	2014-04-06	-5.61	-5.72±0.11	…	…	0.86	0.75±0.11
SCR 1321-1052	2014-04-06	-5.84		…		0.64	
SCR 1421-0916	2014-03-17	+0.08	+0.06±0.01	…	…	0.93	0.93±0.01
SCR 1421-0916	2014-03-17	+0.06		…		0.93	
SCR 1421-0755	2014-03-15	-0.01	-0.01±0.02	…	…	0.91	0.90±0.01
SCR 1421-0755	2014-03-15	+0.02		…		0.88	

Table 6 continued

Table 6 *(continued)*

Designated	Obs	H-α EW (Å)		Li EW (mÅ)		K I EW (Å)	
Name	Date	Measured	Weighted	Measured	Weighted	Measured	Weighted
SCR 1425-4113AB	2013-04-30	-4.76	-4.72±0.05	245	244±1	0.73	0.76±0.03
SCR 1425-4113AB	2013-04-30	-4.66		242		0.79	
SCR 1438-3941	2013-04-30	-0.12	-0.10±0.01	…	…	0.78	0.78±0.01
SCR 1438-3941	2013-04-30	-0.09		…		0.79	
LP 914-6	2013-05-01	-0.18	-0.17±0.01	…	…	1.24	1.23±0.01
LP 914-6	2013-05-01	-0.17		…		1.23	
SCR 1521-2514	2013-05-21	-3.86	-3.84±0.02	…	…	1.06	1.06±0.01
SCR 1521-2514	2013-05-21	-3.82		…		1.06	
SCR 1708-6936	2013-04-28	-4.52	-4.57±0.05	…	…	1.19	1.16±0.04
SCR 1708-6936	2013-04-28	-4.62		…		1.12	
SCR 1816-6305	2013-04-28	-0.02	-0.11±0.08	…	…	0.85	0.91±0.05
SCR 1816-6305	2013-04-28	-0.20		…		0.96	
SCR 1816-6305	2013-04-28	-0.10		…		0.92	
SCR 1842-5554A	2013-08-20	-3.55	-5.54±1.06	…	…	0.86	0.97±0.03
SCR 1842-5554A	2013-08-20	-3.58		…		1.02	
SCR 1842-5554A	2014-03-16	-6.38		…		0.97	
SCR 1842-5554A	2014-03-16	-5.91		…		0.98	
NLTT 47004AB	2013-06-18	-0.11	-0.11±0.01	…	…	0.88	0.88±0.01
NLTT 47004AB	2013-06-18	-0.10		…		0.87	
SCR 1856-6922	2013-04-28	-0.10	-0.08±0.02	…	…	1.02	1.03±0.01
SCR 1856-6922	2013-04-28	-0.06		…		1.04	
WT 625	2013-07-22	-3.98	-3.97±0.01	…	…	1.07	1.06±0.01
WT 625	2013-07-22	-3.96		…		1.06	
SCR 1922-6310	2013-05-18	-4.83	-4.79±0.04	…	…	1.14	1.14±0.01
SCR 1922-6310	2013-05-18	-4.75		…		1.15	
RX 1924-3442	2013-08-20	-10.13	-10.18±0.05	…	…	1.08	1.17±0.09
RX 1924-3442	2013-08-20	-10.23		…		1.27	
SCR 1926-5331	2013-08-20	-2.33	-2.27±0.06	…	…	0.86	0.83±0.02
SCR 1926-5331	2013-08-20	-2.21		…		0.81	
SCR 1938-2416	2013-06-17	-0.46	-0.45±0.01	…	…	1.06	1.05±0.02
SCR 1938-2416	2013-06-17	-0.44		…		1.03	
SCR 1951-4025	2013-06-16	-0.21	-0.27±0.06	…	…	1.00	1.02±0.02
SCR 1951-4025	2013-06-16	-0.33		…		1.04	
SCR 2004-6725A	2013-04-28	-3.50	-3.55±0.04	…	…	0.91	0.91±0.01
SCR 2004-6725A	2013-04-28	-3.58		…		0.91	
2MASS 2004-3356	2014-04-10	-8.50	-8.20±0.15	…	…	1.40	1.26±0.09
2MASS 2004-3356	2014-04-11	-8.16		…		1.30	
2MASS 2004-3356	2014-04-11	-8.09		…		1.16	
SCR 2008-3519	2013-06-16	-5.45	-5.42±0.03	…	…	0.98	0.99±0.01
SCR 2008-3519	2013-06-16	-5.39		…		1.00	
SCR 2010-2801AB	2013-05-23	-7.93	-7.94±0.02	…	…	0.92	0.93±0.01
SCR 2010-2801AB	2013-05-23	-7.97		…		0.94	
L 755-19	2013-06-12	-5.32	-5.35±0.03	…	…	1.29	1.29±0.01
L 755-19	2013-06-12	-5.38		…		1.29	
SCR 2107-7056	2014-07-15	-5.29	-5.31±0.02	…	…	1.18	1.18±0.01
SCR 2107-7056	2014-07-15	-5.34		…		1.18	
SCR 2107-1304	2013-08-22	-4.27	-4.21±0.06	…	…	1.19	1.18±0.01
SCR 2107-1304	2013-08-22	-4.15		…		1.16	
LEHPM 1-4147	2013-04-28	+0.02	+0.01±0.01	…	…	0.86	0.86±0.01
LEHPM 1-4147	2013-04-28	-0.01		…		0.87	

Table 6 continued

Table 6 *(continued)*

Designated	Obs	H-α EW (Å)		Li EW (mÅ)		K I EW (Å)	
Name	Date	Measured	Weighted	Measured	Weighted	Measured	Weighted
SCR 2204-0711	2013-08-23	-0.34	-0.33±0.01	...	...	-0.09	-0.07±0.01
SCR 2204-0711	2013-08-23	-0.32		...		-0.06	
SCR 2237-2622	2013-08-18	-6.24	-6.24±0.05	...	...	1.46	1.46±0.02
SIPS 2258-1104	2013-09-13	-1.80	-1.82±0.01	...	...	1.16	1.16±0.01
SIPS 2258-1104	2013-09-13	-1.83		...		1.16	
LEHPM 1-5404	2013-08-20	-0.08	-0.09±0.01	...	...	0.95	0.95±0.01
LEHPM 1-5404	2013-08-20	-0.09		...		0.94	
SCR 2328-6802	2013-08-20	-3.89	-3.89±0.01	...	...	0.92	0.92±0.01
SCR 2328-6802	2013-08-20	-3.89		...		0.93	
LTT 9582	2013-08-20	-3.79	-3.79±0.01	...	...	1.30	1.29±0.01
LTT 9582	2013-08-20	-3.79		...		1.28	
G 275-71	2013-11-30	-0.06	-0.01±0.02	...	...	0.91	0.94±0.02
G 275-71	2013-11-30	-0.01		...		0.95	
LEHPM 1-6053	2013-08-23	-0.07	-0.06±0.01	...	...	0.94	0.94±0.01
LEHPM 1-6053	2013-08-23	-0.04		...		0.94	
			Flux Standards				
LTT 1020	2014-02-05	+0.03	+0.03±0.01	...	...	-0.92	-0.92±0.02
EG 21	2013-08-21	+0.53	+0.40±0.30	...	...	-0.05	-0.03±0.05
EG 21	2013-12-01	+0.52		...		-0.14	
EG 21	2014-01-17	-0.13		...		0.04	
EG 21	2014-01-18	+0.64		...		0.00	
LTT 2415	2013-04-30	-0.78	-0.78±0.02	...	...	-0.05	-0.05±0.02
HILTNER 600	2014-03-08	-0.00	-0.00±0.01	...	...	0.08	0.08±0.01
LTT 4364	2013-06-18	+0.01	+0.02±0.01	...	...	0.01	-0.39±0.51
LTT 4364	2013-06-18	+0.02		...		-1.04	
LTT 4364	2014-01-14	+0.01		...		-0.02	
HR 5501	2014-03-15	+0.97	+0.97±0.01	...	...	-0.01	-0.01±0.01
LTT 7987	2014-04-06	+0.18	+0.18±0.03	...	...	0.04	0.04±0.04